World Climate Congress 2021

Visnav

World Climate Congress 2021

Organized by

Bagmati UNESCO Club

&

Gandaki UNESCO Club

On

22nd and 23rd July 2021

Published by

International Journal of Applied Chemical and Biological Sciences

ISSN: 2582-788X

Visnav

World Climate Congress 2021
International Journal of Applied Chemical and Biological Sciences
ISSN: 2582-788X

ORGANIZING TEAM

Bagmati UNESCO Club

Nishchal Baniya
• President

Bidhan Shrestha
• Vice President

Pratistha Dhakal
• General Secretary

Sakar Mainali
• Treasurer

Rajan Katuwal
• Media Coordinator

Rojan Sapkota
• Chief, Environment Section

Debesh Mahat
• Chief, Health Section

Shubhashis Bhattarai
• DY. Chief

Pratik Baral
• DY. Chief, Environment Section

Ashim Subedi
• Executive Director

Nimesh Timalsina
• HR Manager

Arun Karki
• Member

Aastha Aryal
• Member

World Climate Congress 2021
International Journal of Applied Chemical and Biological Sciences
ISSN: 2582-788X

ORGANIZING TEAM

Gandaki UNESCO Club

Dikchit Parajuli
- President

Sabnam Subedi
- Vice President

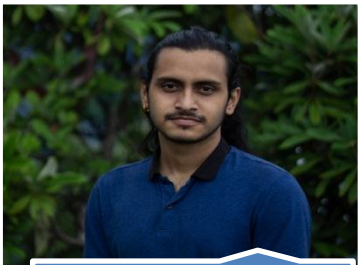

Nischal Poudel
- Secretary

Sweta Ranabhat
- DY. Secretary

Swikriti Adhikari
- Director of Finance

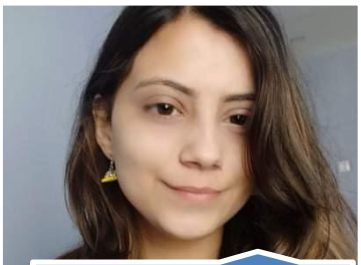

Rojina Bhattarai
- Chief, International Relations

Suraj Chaurasiya
- Member

Rasmita Sapkota
- Member

INDEX

World Climate Congress 2021
International Journal of Applied Chemical and Biological Sciences
ISSN: 2582-788X

Full Length Paper

World Climate Congress 2021
International Journal of Applied Chemical and Biological Sciences
ISSN: 2582-788X

PUTTING THE CRISIS IN CLIMATE CRISIS

Angela Zhong *

Harvard College, Faculty of Arts and Sciences, Cambridge, MA 02138

* For correspondence: ayzhong@college.harvard.edu

Abstract

In the present study, the author conducts a literature review and analysis of the impact of climate change on international security. This is especially pertinent at a time where environmental problems are being securitized by national bodies. Due to the sheer number of secondary and tertiary effects of climate change on international security, the paper focuses on defending an expansive understanding of security and delving into resource wars and border conflicts. The paper concludes with suggestions for a hybrid model of climate governance.

Keywords: border, conflict, international security, resource

1. INTRODUCTION

It is no secret that there are catastrophic effects from climate change; there have been many climate change-based disaster scenes portrayed in Hollywood, spawning a genre known as “cli-fi” or climate fiction that ranges from dystopias like Snowpiercer and apocalypses like The Day After Tomorrow to satire like Sharknado 2 (Yale Climate Connections). Despite the oversaturation of “climate pornography” in mainstream media, one area of academia that has not adequately entered the attention of the public is climate change’s impact on international security, something that could be argued is more terrifying than Interstellar (Atkin). After evaluating dozens of security-related climate change concerns that are prominent in the status quo, I have narrowed the focus down to two groups of personal interest for the purposes of depth

and length: border conflicts and resource wars. Others that I also considered included: transmittable disease, renewable energy sources, etc. Academically, I will illustrate later in the paper that these two selections are also some of the most obvious and on-going concerns for state security, making this paper a particularly relevant primer.

In this paper, I will first clarify a few of the direct consequences of climate change and how they relate to the two security scenarios listed above. I will then discuss any potential solutions to end border conflicts and resource wars respectively and why these options may be promising or fail in different circumstances.

2. DIRECT CONSEQUENCES OF CLIMATE CHANGE

According to the Intergovernmental Panel on Climate Change (IPCC) of the United Nations (UN), the global average temperature is expected to increase by 1.5℃ (around 2.7°F) by 2040 due to human activity. The rigorous climate models predict that the expansion may even reach 2℃, approximately 3.6°F. This is not to say there is no dispute on the issue; though the IPCC is the internationally accepted authority on climate change, many have criticized the IPCC for being too conservative and only considering the lowest common denominator that most of the literature would agree to. Though the change may seem incremental to us Bostonians who must adapt to 60°F temperature variances, even the mildest prediction, 1.5℃ addition to the global average temperature, would generate rippling results.

3. PHYSICAL EFFECTS

There is a litany of direct impacts that materialize from climate change's higher average surface and ocean temperatures. Here, I have outlined and provided examples of three of the countless ramifications: a rise in sea levels, increased rainfall, increased frequency and intensity of extreme weather conditions.

Scientists predict with medium confidence that that (1) sea levels will rise up to .77m by 2100 with a 1.5℃ increase (UN). This is because more of the continental ice fields reach their melting point with the increased temperatures (Purvis and Busby). This is not something that will begin when the 1.5℃ mark is reached but rather is already happening and will continue to happen even with a decrease in emissions (Moens). The 1.5℃ indicator

simply acts as a benchmark for the increased rate of growth.

Additionally, with the increase in water content that was originally stored in ice, there will be more water that can be evaporated. In fact, for every 1°F rise in the global average temperature, the atmosphere is able to hold four percent more water vapor than originally (Climate Central). Paired with the hotter mean conditions, increased evaporation is expected to produce (2) more rainfall (Climate Central). In my hometown of Houston, Texas, for instance, the wettest day of the year has grown more than 2.78 inches in the past seventy years (Climate Central). The wider range in rainfall and temperatures raises the (3) frequency and intensity of extreme weather events such as tornadoes, floods, droughts, hurricanes, etc (Climate Central). Climate Central explains that "Hurricane Harvey made the record rain in Houston at least three times more likely and 15% more intense."

However, it is unlikely that the impacts of climate change are distributed evenly. For example, increased flooding is particularly intrusive for "small islands, low-lying coastal areas and deltas" whose residents are inherently surrounded by water and have no place to run (IPCC). For instance, "over 80% of the land area have less than one meter above mean sea level, climate change and its associated sea level rise would undoubtedly be a catastrophe and threaten the livelihood of the islanders in the Maldives alike many thousands of others in low-lying island states," according to Abdullahi Majeed, State Minister of Energy and Environment. Thus, it is important to acknowledge the regional differences in climate change impacts to international security, which will be the focus of the next section.

4. SECURITY IMPACTS OF CLIMATE CHANGE

Now that readers have a baseline understanding of some of climate change's consequences, the repercussions can be tied to the second-order security concerns. This is an area that should be of immense concern to policymakers as the United Nations International Strategy for Disaster Reduction finds that at least 1.692 billion people were affected by natural disasters between 1990 and 1999, six times more than those affected by armed conflict during the time period. Furthermore, disasters between 1998 and 2017

generated $2.908 trillion USD in losses (UNISDR).

With climate change having more widespread shocks on security than war itself, it is important to define what it means to have international security. For the following sections, I adopt the United Nations Development Programme (UNDP) 1994 Human Development Report's definition of security, which provides a more expansive understanding that puts "environmental security" -- and therefore the human-generated influences in climate change -- at the forefront of the analysis. Futamura *et al* explain, Whereas a traditional understanding of security emphasizes the military defense of state interests, human security provides an alternative, human-centered perspective that focuses on securing and protecting individuals' "freedom from want" and "freedom from fear". It offers a broader understanding of security, by incorporating concerns of development and human rights as well as more traditional issues.

This clarity enables actors to more easily imagine resolution that does not involve military action. Currently, the rhetoric surrounding climate change and security that many United States senior officials advance lends itself to further militarization. The military wants to prevent its resources from being diverted to foreign aid, but that does not have to be the case, as I discuss in the next section (Futamara *et al*).

With this precision, we can move on to discuss some of the ways that the climate crisis affects governments' abilities and obligations to keep their constituents safe. It is important to note that the following analysis is not a one-to-one relationship between cause and effect since many of these causes are able to generate the same outcome.

4.1. Resource Conflicts: Military Violence

Another area of concern is in the diminishing of resources as "disputes over limited natural resources have played at least some role in 40 percent of all intrastate conflicts in the last 60 years" (King and Burnell). In arid and semi-arid regions like the Middle Eastern and North African states, the water supply, quality, and accessibility are all becoming a source of tension as the warmer temperatures produce drier overall climates and unexpected droughts. This stressor is only worsening with the internal migration that

was described earlier. Though water scarcity has traditionally been an area that nations collaborated on for common goals, "the US intelligence community suggests that states may begin employing water as an interstate 'weapon,' even in areas where cooperative solutions had prevailed." Rogue actors have already begun this trend. In late 2014, the Islamic State (IS) gained control of the Mosul dam and threatened Mosul and Baghdad with a flood, which prompted Iraqi, Kurdish, and US militaries to begin aerial bombing IS (King and Burnell). IS later diverted water from nearby rivers, preventing the advancement of Iraqi forces multiple times (King and Burnell). King and Burnell write that, in scenarios like these, a positive feedback loop is created where more agents are desperate to gain control of the resource, thereby creating more overall conflict in the long run (King and Burnell). Though water is a commodity in the Middle East and in North Africa, most countries that rely on exports of biological commodities face parallel problems. Coffee in Guatemala, El Salvador and Honduras (Fetzek), and fishing patterns in the South China Sea (SCS), the Arctic, and the African great lakes have also generated similar friction (Thomas).

Resource "wars" have been a source of contention for millennia, but climate change has accelerated the levels of scarcity far faster than ever before and is expected to continue to increase (King and Burnell). This is not to say that scarcity is an absolute concern; in much of the developed world, water, coffee, and fish are plentiful due to institutionalized plunder for resources. Though the planet only consists of one percent freshwater that is readily available for use, if evenly distributed, it would be more than enough for the current world population. Instead, it is concentrated in a way that excludes many developing nations (UN Water). Thus, one proposal to resolve resource wars that is becoming more popular is to address the root causes of the violence (lack of secure resources, for one) via peacebuilding. Peacebuilding efforts combine development and security by developing positive peace absent the need for better living conditions (Swain). For water-based negative conflict, this could include: "legal reforms and building of sound water institutions; careful planning of water use to achieve sustainable food security; and cooperative involvement of international, national and local stakeholders in the planning and managing

of water resources" (Swain). Environmental peacebuilding has been considered as a more effective and less violent approach to resource wars (Swain) but has limited applicability in addressing the brunt of terrorism, where ideology, social strata, and other sociological factors also play a driving role (Bjorgo). Nevertheless, the acknowledgement that these complex socioeconomic worries cross disciplinary boundaries is a landmark move away from traditionally militarized attacks of climate change writ-large (Ide *et al*).

4.2. Resource Conflicts: Territorial Encroachment

A dearth of consistent water supply can spark violence in less militaristic settings as well. Many herdsmen in Nigeria's once rich Middle Belt depend on grazing lands for their agricultural pursuits (Ide *et al*). As the region becomes drier, their cattle must move farther out for the same sustenance (Ide *et a*l). This means their animals can encroach on the territory of other farmers or trample over landowners' produce (Ide *et al*). Though these disputes may seem inconsequential, desperation abounds. "In 2016, herdsman killed more Nigerians than Boko Haram, the extremist group widely considered the primary threat to Nigerian security" (Ide et al). With these ongoing battles, it also makes it more difficult for the government to establish consistent and enforceable rules regarding land rights (Ide et al). This is a great example of how peacebuilding could be effectively applied to (re-)promote collaboration and conflict resolution within the region rather than further escalation by national or international players. Empirically, peacebuilding has been successfully used via tara bandu in post-civil war Timor-Leste as a bottom-up approach. "Local communities use this ritual practice to manage natural resources, social conflicts and spiritual relations at the same time" (Ide et al).

4.3. Resource Conflicts: Natural Disasters

The lack of resources available is only exacerbated by natural disasters like the 2010 Haitian earthquake to Australia's bushfires the year previously to the 2004 Indian Ocean tsunami (Ide *et al*). Many residents who suffer through these catastrophes may become what is known in the media as "climate refugees," sparking a wave of xenophobia and right-wing populism (Podesta). Some argue that

the host countries are already strained for resources for their own citizens, much less immigrants. However, politically charged headlines often skim over the nuances of the phenomenon. While most manifestations of climate change do exacerbate existing conditions, they are generally not the sole cause of immigration now, though that could quickly change in the upcoming years (Podesta). People who are struck by natural disasters and move are most likely internally displaced persons (IDP) or "environmental migrants," meaning they do not cross state lines (Podesta). Many are located near "South Asia, Central America, Northwest Africa, and the Horn of Africa" (Podesta). The approximately 21.5 million IDPs are not designated as refugees by the United Nations, and thus do not receive the same legal support that the classification provides due to a lack of resources and direction (Podesta).

In the future, multilateral institutions, development agencies, and international law is expected to continue to convene for agreements like the The Global Compact for Safe, Orderly, and Regular Migration or Warsaw International Mechanism for Loss and Damage Associated with Climate Change (WIM) recommendations. Unfortunately, these have not been binding thus far and will require more initiative and effort to ensure that countries comply (Podesta). This is in part due to the free rider problem and the financial incentives against mitigating climate change and taking in more disadvantaged people. To overcome such problems fundamentally requires a more cosmopolitan approach to who governments should serve. Peacebuilding and the associated human-centered definition of security is thus key in recognizing the innate imbalance of resources that influence conflict, a prerequisite for international environmental justice.

5. BORDER CONFLICTS

As mentioned in the introduction, one area of existential concern for low-lying island nations is the rising sea levels; families have been forced to flee to other countries after their islands were submerged, creating some of the first legally disputed cases of immigration generated solely from climate change (Podesta). This issue is shared by Kiribati and the Marshall Islands in the Pacific as well as the Maldives in the Indian Ocean (Podesta).

The conundrum of shifting borders is not isolated to small, low-lying island states

either. Many geopolitical superpowers like the United States have also been mulling over their next steps (King and Burnell). Roblin furthers,

A 2019 report by the Pentagon concluded that 79 military bases will be affected by rising sea levels and frequent flooding. The largest naval base on the planet, located in Norfolk, Virginia, may become unusable due to flooding caused by a rising sea level and more frequent hurricanes — threatening to take out the home port of six aircraft carriers. Island bases, including a missile test range and a billion-dollar air defense radar, risk becoming uninhabitable due to flooding and saltwater contamination.

However, this distress about saltwater intrusion is predictable in a way that flash floods are not. Islands take time to slowly be submerged, allowing for the adaptation of status quo understandings of sovereignty and borders (King and Burnell).

Currently, under the United Nations Convention on the Law of the Sea (UNCLOS) Article 21, islands have rights up to 200 miles into the sea as long as these regions are habitable. That radius extends from a baseline point above sea level and empowers the country with the property rights for anything within that area: reefs, fisheries, deep-sea deposits, etc. With the rising levels, parts of countries -- especially archipelagos -- may no longer be classified as islands but instead as “rocks” without those same rights to an Exclusive Economic Zone (EEZ) even before they are permanently submerged (King and Burnell). Thus, other countries would legally be permitted to encroach on those resources. Island nations are using Article 7 of UNCLOS to amend the policy by submitting permanent boundaries that will not change with the shifting sea patterns (King and Burnell). This solution is by no means perfect though. It is simply a band-aid over a bullet wound from the perspective of the thousands of residents who live near the coast -- it does not address the root cause of the problem. From the standpoint of international law, this maneuver has no precedence either. Both directions of opposition are perfectly legitimate and should be rectified immediately. However, until there is a better proposal, the permanent revision of boundaries may be able to mitigate future border conflicts for nations who are concerned with sea levels specifically (King and Burnell).

6. CONCLUSION

In conclusion, there are many layers of climate change that policymakers, consumers, and diplomats should evaluate. Just because rising sea levels may not affect the Great Plains the same way that it would Tokyo does not mean that the residents of South Dakota will not intimately feel the financial aftermath or face crippling droughts. On one hand, a focus on adapting to the most material, direct outcomes of the climate crisis can ignore other problems that spring from environmental degradation, foreclosing the potential of effective reform. On the other hand, purely theoretical talks of emissions can also alienate those who suffer under security threats in the status quo. Only by taking a holistic approach to security can actors generate innovative solutions to the most pressing issues of our time. This requires a strict evaluation of the different regional (cultural, environmental, social, political, economical) factors that shape responses to climate change and an awareness that a one-size fits all approach does not make sense. To universally mandate that countries engage in peacebuilding activities or codify legal agreements is to paper over the historical injustices that have ravaged the global South. Instead, a hybrid approach where there is a top-down initiative to mitigate climate change directly as well as bottom-up grassroots coalitions of conflict resolution seem to be the most ideal way of including all stakeholders. Society can then tackle the root cause and nurse the symptoms with context and cultural understanding.

7. ACKNOWLEDGEMENT

I am incredibly grateful to my professor, Dr. McElroy from the Harvard Environmental Science Public Policy Department, for the opportunity to delve into a topic of my choosing for the final assignment. His words of encouragement were instrumental in my confidence to submit this paper. I have discovered my passion for the environment in large part due to the scintillating discussions I had in his class, especially under the guidance of the teaching fellows.

8. CONFLICT OF INTEREST

The author declares no conflicts of interest.

9. SOURCE(S) OF FUNDING

The author did not require funding.

10. REFERENCES

1. Atkin, Emily. (2017). The Power and Peril of Climate Disaster Porn, The New Republic, https://newrepublic.com/article/143788/power-peril-climate-disaster-porn
2. Bjørgo, Tore. (2019). Root Causes of Terrorism. Routledge Taylor & Francis Group, https://opev.org/wp-content/uploads/2019/10/BJ%C3%98RGO-Tore.-Root-Causes-of-Terrorism-.pdf
3. Cli-Fi Movies: A Guide for Socially-Distanced Viewers, Yale Climate Connections, 2019, https://yaleclimateconnections.org/dl/YCC_Cli_Fi_Listing.pdf
4. Climate Change Small Island Developing States. (2005). United Nations Framework Convention on Climate Change (UNFCCC) https://unfccc.int/resource/docs/publications/cc_sids.pdf
5. Coping with water scarcity. (2007). Challenge of the twenty-first century. UN-Water, https://www.un.org/waterforlifedecade/scarcity.shtml
6. Disasters: UN report shows climate change causing 'dramatic rise' in economic losses. (2018). UN Office for Disaster Risk Reduction (UNISDR). https://news.un.org/en/story/2018/10/1022722
7. Fetzek, Shiloh. (2017). Climate Coffee and Security, Epicenters Of Climate And Security, https://climateandsecurity.files.wordpress.com/2017/06/epicenters-of-climate-and-security_the-new-geostrategic-landscape-of-the-anthropocene_2017_06_091.pdf
8. Futamara, Madoka et al. (2011). Natural Disasters and Human Security. United Nations University. https://unu.edu/publications/articles/natural-disasters-and-human-security.html
9. Ide, T., Bruch C., Carius A., Conca K., Dabelko G.D., Matthew R., Weinthal E. (2021). The past and future(s) of environmental peacebuilding, International Affairs, Volume 97, Issue 1, Pages 1–16, https://doi.org/10.1093/ia/iiaa177
10. King, Marcus and Burnell, Julia. (2017). The Weaponization of Water in a Changing Climate. Epicenters Of Climate And Security, https://climateandsecurity.files.wordpress.com/2017/06/epicenters-of-

climate-and-security_the-new-geostrategic-landscape-of-the-anthropocene_2017_06_091.pdf

11. Moens, Jonathan. (2020). Andes Meltdown: New Insights Into Rapidly Retreating Glaciers. Yale Environment 360, https://e360.yale.edu/features/andes-meltdown-new-insights-into-rapidly-retreating-glaciers
12. Pouring It On: How Climate Change Intensifies Heavy Rain Events. (2019). Climate Central, https://www.climatecentral.org/news/report-pouring-it-on-climate-change-intensifies-heavy-rain-events
13. Purvis, Nigel And Busby, Joshua. (2004). The Security Implications Of Climate Change For The UN System. The Wilson Center Environmental Change and Security Program, https://citeseerx.ist.psu.edu/viewdoc/download?doi=10.1.1.585.9041&rep=rep1&type=pdf
14. Roblin, Sebastian. (2020). The U.S. military is terrified of climate change. It's done more damage than Iranian missiles, NBC News, https://www.nbcnews.com/think/opinion/u-s-military-terrified-climate-change-it-s-done-more-ncna1240484
15. Summary for Policymakers. (2018). IPCC. In Press.
16. Swain, Ashok. (2016). Water and post-conflict peacebuilding. Hydrological Sciences Journal, 61:7, 1313-1322, DOI: 10.1080/02626667.2015.1081390
17. Thomas, Michael. (2017). Fish and Conflict. Epicenters Of Climate And Security, https://climateandsecurity.files.wordpress.com/2017/06/epicenters-of-climate-and-security_the-new-geostrategic-landscape-of-the-anthropocene_2017_06_091.pdf

World Climate Congress 2021
International Journal of Applied Chemical and Biological Sciences
ISSN: 2582-788X

DEEP LEARNING FOR FOREST MANAGEMENT: DEAD TREE DETECTION AND SEGMENTATION FROM RGB AERIAL IMAGES

Arogya Dahal, Kalyan Khatiwada, Siddhartha Gautam *

Kathmandu, Nepal

* For correspondence: gsiddhartha63@gmail.com

Abstract

The increasing number of forest fires in different parts of the world exacerbates climate change through a positive feedback loop. The emission of greenhouse gases from forest fires accelerates climate change, reinforcing tree mortality that results in even larger eruptions of forest fires. This cycle has to be broken by formulating a forest management plan that focuses on the management of the dead trees. Traditionally, expensive datasets like RGBI images have been used to detect and survey dead trees in forests. This research aims to determine a method to locate dead trees using economical RGB datasets and a more convenient machine learning model. The segmentation model that we trained on the RGB data set detects dead trees in images with higher accuracy of 95.8 %. Our results enable forest service agencies to understand and analyze the situation of dead trees in their forest without worrying about cost and complexity.

Keywords: datasets, forest management, RGB

1. INTRODUCTION

Tree mortality has both beneficial effects and detrimental effects. The major causes of tree mortality in most forests are drought, beetle infestation, diseases and high tree densities. While the dead trees are essential to the functioning of ecosystems [1], they also act as fuel for forest fires and result in a greater spread [2].

On January 5 of 2021, The capital of Nepal, Kathmandu, witnessed its air

quality index (AQI) rise to the record high value of 500. AQI value below 50 represents good air quality [3]. The decline in quality resulted from the emission of dangerous gases such as carbon monoxide, nitrogen dioxide, formaldehyde, and acetaldehydes from the forest fires [4]. Dead trees in those forests played a pivotal part in the rise and acceleration of the forest fires. Due to the increasing number of dead trees, the scale of forest fire increases. Subsequently, more carbon emission occurs accelerating climate change which in turn increases the rate of tree mortality prompting a positive feedback loop.

To control the cycle, a method is required to suppress the stimulus provided by dead trees in forests. Hence, an identification of dead trees in forests is necessary. The data currently required for the estimation is too expensive to collect, especially for developing countries like Nepal. In this project, we attempt to determine a convenient and economical way of detecting dead trees.

We train an instance segmentation model on our custom dataset which consists of RGB aerial images of forests from several geographical areas within the US. This approach results in a model capable of identifying dead trees under diverse circumstances. The utility of the model is then validated by testing it on images from two different areas. The main advantage of the project is the simplified pattern of data collection and evaluation for the identification of dead trees.

Based on the results of this work, the number of dead trees can be estimated. Using these estimates, forest management agencies can work on measures to reduce the number of dead trees in order to control the influence it has on forest fires.

Generally, satellite imagery has been used to identify the loss of forest cover, and measure the biophysical changes of forest over time. Sylvian (2019) [5] had used CNN based neural network to detect dead trees from RGBI image dataset and had suggested on using semantic segmentation models. Jiang (2019) [6] used a semantic segmentation based model to detect and segment dead trees from aerial imagery; 4 channel RGBI image was used as the input to the model. In a recent study, Chiang *et al* (2020) [7] used an instance segmentation based model to detect dead trees from RGB aerial imagery, achieving a maximum of 0.60 bounding box

mAP@50 score when trained on 3600 images for 100 epochs.

The previous studies either used VHR CIR (Very High Resolution Color-Infrared Imagery) or high resolution near ground level aerial imagery to create their dataset. The use of the former technique during the training phase limits the scope of the study as acquisition of RGBI train/test set is expensive as compared to RGB dataset. The use of the latter technique makes the labeling of data tedious and creates data scarcity. Chiang *et. al*. used synthetic data creation technique to surmount data scarcity; however, some disadvantages of this technique were highlighted by the authors. We build on top of their experiences and aim to provide the best of both techniques. To overcome both the problems simultaneously, we created our data from RGB aerial imagery provided by public sources. Our training and test datasets contain variance with respect to geography, climate and species of trees.

2. METHODS AND MATERIALS

2.1. Dataset Details

The dataset was created using RBG aerial images from the Google Earth Engine8. (RGB aerial images are easily available in the internet sources like Google Maps and such, unlike RGBI images.).The training dataset is collected from various states of the United States (Table 1, Figure 2), especially, but not limited to, New Hampshire, and Maine. These regions were chosen because of their high percentage of forest coverage. The images were initially obtained in 1920 x 1080 resolution, each of which were then divided into 6 x 4 grid each of size 320 x 270 accelerating the training. The processed images were then separated into two groups: one containing dead trees and another with no dead trees. The images containing dead trees were labelled and the x and y coordinates of the target object were stored in COCO format annotation file [7]. We have a total of 350 images in the training set and 50 images in the validation set.

The test set was created from aerial images of two sites: Soquel Demonstration Forest, California and New River Gorge National forest, West Virginia. All of the images from these two sites were processed with the previously mentioned method. The test set consists of 2904 processed images from two different sites covering an area of approximately 80km [2].

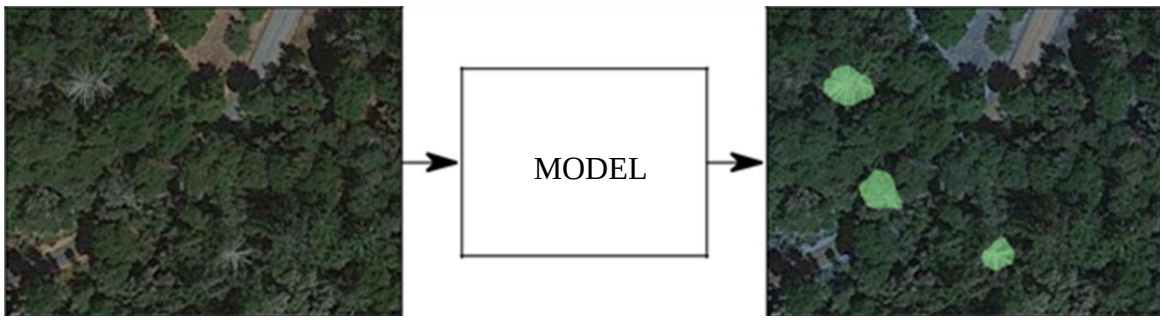

Figure 1. From left to right, RGB images get passed to the model which segments and counts dead trees from the images.

2.2. Model

We experimented with two different object segmentation approaches: semantic segmentation and instance segmentation. We trained two different segmentation models on our dataset: U-Net [13] and DeepLabv3 [7]. Although being slightly faster, both models produced segmentation masks that were larger than the ground truth. Moreover, the segmentation mask suffered from false positives on the test set.

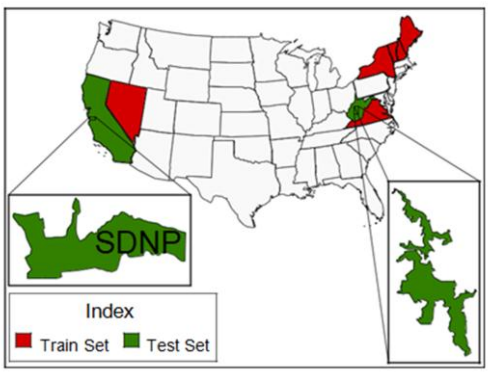

Figure 2. Dataset composition distribution on the basis of states; Red represents train set distribution; Green represents test set distribution.

An instance segmentation model, although slightly slower, performed much better than semantic segmentation models.

The segmentation masks from it were closer to the ground truth labels and the rate of false positive on the test set decreased drastically. We used Swin Transformer Model [12] as the backbone and Mask RCNN [9] as the classifier head. Both the backbone and the classifier head were pre-trained on ImageNet dataset. We used a cross-entropy loss function and mask loss during the training phase. AdamW was employed using a cosine decay learning rate.

Scheduler with initial learning rate 0.001, beta values 0.9 and 0.999 and a weight decay of 0.05. The model was trained for 100 epochs on NVIDIA Tesla K80 GPU; however, the improvement after epoch 35

Table 1. Major Forest Type in States from the dataset and their composition percentage

States	Forest Type	% In Dataset	Train
Nh	Beech-Maple	40.3	√
Me	Decidious Hw	39.3	√
Vt	Taiga	6.3	√
Ny	Beech-Maple	6.4	√
Va	Oak-Hickory	5.4	√
Nv	Pinyon/Junipe	2.3	√
Wv	Redwood	89.26	×
Ca	Oak-Hickory	10.73	×

was minimal. During testing, the convolution layer and the batch normalization layers were fused. This was done to save computational resources and at the same time simplify the network architecture.

3. RESULTS AND DISCUSSIONS

Figure 5 illustrates the loss of the model during the training phase. The model was trained for 35 epochs only as any further training did not result in significant improvements. Figure 5 demonstrates the graph of evaluation metrics on the validation set. The model achieves a maximum of 0.724 on segmentation mAP

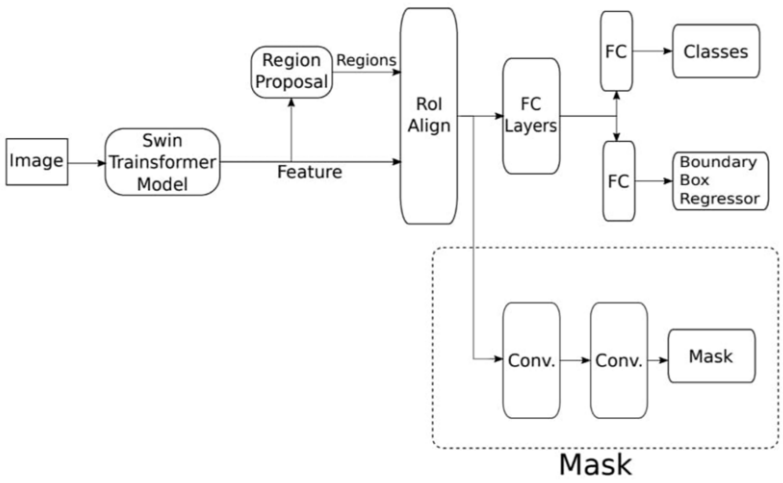

Figure 3. Structure of the Model Pipeline; Swin Transformer Model acts as the backbone for the model whose features maps get passed on to the Mask RCNN classifier head.

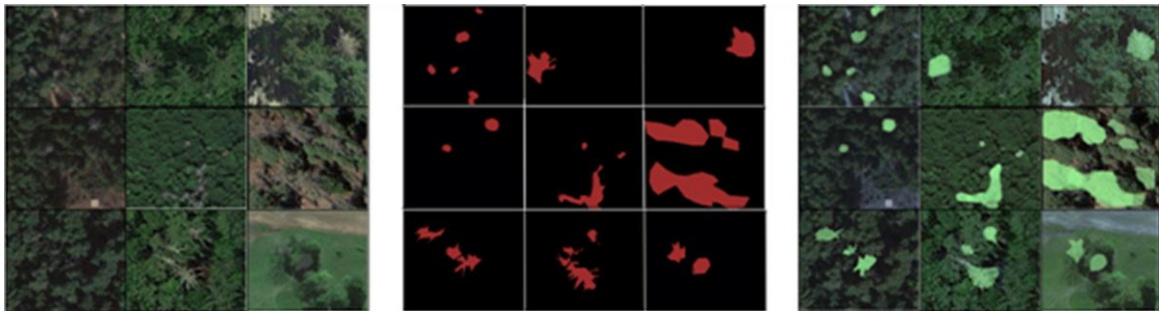

(a) (b) (c)

Figure 4. (a) shows the RGB image obtained after processing; (b) shows the hand labeled segmentation mask; (c) shows the segmentation mask as predicted by the trained model. The first column shows images from New River Gorge National Park, second column shows images from Soquel Demonstration State Forest. Top to bottom, third column shows images from NH, VT and ME.

score and 0.683 on bounding box mAP score for an IoU threshold of 0.50.

The applicability of these results are then tested on images from our test set. These images were fed to the model, which was tasked to separate images containing and not containing dead trees and to segment dead trees from the images. The summary of the predicting result on the classification problem is shown on the confusion matrix in Figure 6

This shows that our trained model performs well on the task of identifying images containing dead trees with an

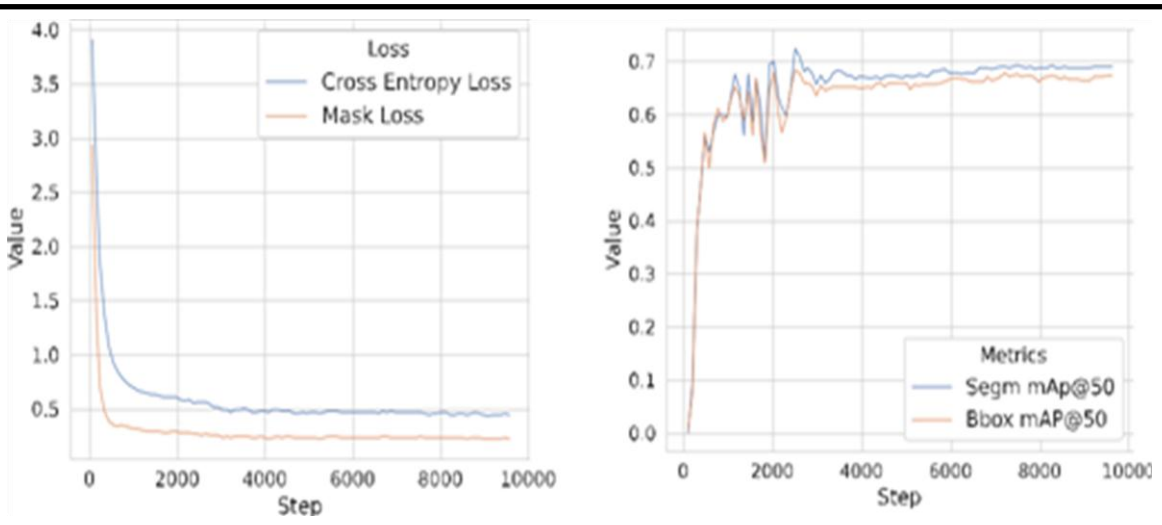

(a) (b)

Figure 5. (a) and (b) illustrates the loss and accuracy of the model during the training and validation phase respectively.

n = 2904		Predicted Class: Positive	Predicted Class: Negative	
Actual Class	Positive	1269 (44.621%)	78 (0.027%)	Recall 0.942
	Negative	44 (0.015%)	1512 (52.066%)	Specificity 0.972
		Precision 0.966	Negative Predictive Value 0.951	Accuracy 0.958

Figure 6. Confusion Matrix for the combined test set; Positive denote images containing dead trees; Negative denote images not containing dead trees.

accuracy of around 95.8%.

In this research, we develop a convenient and cheap method of detecting dead trees. The results indicate that our method detects dead trees with high confidence. The evaluation metrics showed better result than prior studies using RGB aerial images [6].

We identify a number of limitations of our model. Although our model performs well detecting dead trees of large sizes, it fails to detect dead trees of small sizes. Our model cannot detect dead trees during winter when all the trees are covered in snow. It may also misidentify rare tree species having white leaves. It can be addressed by training the model to categorize the tree species before detecting the dead trees.

Further research can be done in order to analyze the complex effect that dead trees has on the forest fire. The correlation between dead organic matter that is present on forest floors, which serves as fuel in the case of fires, and the number of dead trees that can be identified with our methods could also be addressed with additional research. By training the model with more data, dead trees of most forests could be detected and the method could be used on a global scale.

This research is relevant to a wide range of possible real world applications. Forest management agencies that cannot afford expensive datasets like RGBI images can use this method for estimation of the dead trees in any forest. This will aid them in creating management plans to remove

dead trees in the forests and minimize their risk of acting as fuel for forest fire. Such measures can help to reduce the scale of forest fires and consequently, help in climate change mitigation.

4. CONCLUSION

In conclusion, our research has resulted in a machine learning model that can detect dead trees from aerial RGB images with an accuracy of 95.8%. A forest management plan can be initiated based on the information provided by our model, allowing the positive feedback loop caused by the presence of dead trees to be broken. In this way, this research can aid in alleviating both the dangers of forest fires and climate change.

5. ACKNOWLEDGEMENT

We cannot express enough gratitude to our mentor, Dr. Michael Mommert, senior researcher at University of St. Gallen, for his continued guidance through our research and also ICML 2021 Climate Change Workshop for providing us with the mentorship opportunity.

6. CONFLICT OF INTEREST

We certify that we have NO affiliations with or involvement in any organization or entity with any financial interest (such as honoraria; educational grants; participation in speakers' bureaus; membership, employment, consultancies, stock ownership, or other equity interest; and expert testimony or patent-licensing arrangements), or non-financial interest (such as personal or professional relationships, affiliations, knowledge or beliefs) in the subject matter or materials discussed in this paper.

7. SOURCE(S) OF FUNDING

We did an independent research while using the resources that were freely available and are not backed by any entity with financial interest.

8. REFERENCES

1. Tomescu, R., Tarziu, D. R., and Turcu, D. O. The importance of dead wood in the forest. ProEnvironment Promediu, 4(7), 2011.
2. Stephens, S. L., Collins, B. M., Fettig, C. J., Finney, M. A., Hoffman, C. M., Knapp, E. E., North, M. P., Safford, H., and Wayman, R. B. Drought, Tree Mortality, and Wildfire in Forests Adapted to Frequent Fire. BioScience, 68(2):77–88, 01 2018.

3. Fitz-Simons, T. Guideline for reporting of daily air quality: ir quality index (aqi). 7 1999.
4. Lazaridis, M., Latos, M., Aleksandropoulou, V., Hov, Ø., Papayannis, A., and Tørseth, K. Contribution of forest fire emissions to atmospheric pollution in greece. Air quality, atmosphere & health, 1(3):143–158, 2008.
5. Sylvain, J.-D., Drolet, G., and Brown, N. Mapping dead forest cover using a deep convolutional neural network and digital aerial photography. ISPRS Journal of Photogrammetry and Remote Sensing, 156:14–26, 2019.
6. Chiang, C.-Y., Barnes, C., Angelov, P., and Jiang, R. Deep learning-based automated forest health diagnosis from aerial images. IEEE Access, 8:144064–144076, 2020.
7. Chen, L.-C., Papandreou, G., Schroff, F., and Adam, H. Rethinking atrous convolution for semantic image segmentation., 2017.
8. Gorelick, N., Hancher, M., Dixon, M., Ilyushchenko, S., Thau, D., and Moore, R. Google earth engine: Planetaryscale geospatial analysis for everyone. Remote Sensing of Environment, 2017. doi: 10.1016/j.rse.2017.06.031. URL https://doi.org/10.1016/j.rse. 2017.06.031.
9. Hu, H., Gu, J., Zhang, Z., Dai, J., and Wei, Y. Relation networks for object detection. In Proceedings of the IEEE Conference on Computer Vision and Pattern Recognition, pp. 3588–3597, 2018.
10. Jiang, S., Yao, W., and Heurich, M. Dead wood detection based on semantic segmentation of vhr aerial cir imagery using optimized fcn-densenet. International Archives of the Photogrammetry, Remote Sensing & Spatial Information Sciences, 2019.
11. Lin, T.-Y., Maire, M., Belongie, S., Hays, J., Perona, P., Ramanan, D., Dollar, P., and Zitnick, C. L. Microsoft coco: ´ Common objects in context. In European conference on computer vision, pp. 740–755. Springer, 2014.
12. Liu, Z., Lin, Y., Cao, Y., Hu, H., Wei, Y., Zhang, Z., Lin, S., and Guo, B. Swin transformer: Hierarchical vision transformer using shifted windows, 2021.
13. Ronneberger, O., Fischer, P., and Brox, T. U-net: Convolutional networks for biomedical image

segmentation. In International Conference on Medical image computing and computer-assisted intervention, pp. 234–241. Springer, 2015.

World Climate Congress 2021
International Journal of Applied Chemical and Biological Sciences
ISSN: 2582-788X

REVIEW OF FIBROUS FILTER BED MASK DESIGN

Awanish Adhikari [1]*, Sabin Dotel [1], Pratik Baral [1], Udip Adhikari [2]

[1] Department of Environmental Science and Engineering, Kathmandu University, Nepal
[2] Department of Physics, Kathmandu University, Nepal

* For correspondence: awanishadhikari10@gmail.com

Abstract

Masks have consistently been identified as an effective tool against environmental threats. They are considered as protective equipment to preserve the respiratory system against non-desirable air droplets and aerosols such as viral or pollution particles. The filtration efficiency of the different masks against these aerosols is not the same, as the particles have different sizes, shapes, and properties. In this paper, the literature about the different kinds of face masks has been reviewed. In addition, the associated mechanisms of penetrating aerosols through masks are discussed. Finally, the cost of a simple fibrous filter bed mask was determined.

Keywords: face mask, fibrous bed

1. INTRODUCTION

We are currently living in a time when covid-19 is already causing the infection of more than 2.5 million people and more than 300,000 deaths worldwide. In this situation to protect the population, an effective solution is an individual containment; it is the use of a high-performance mask. The main purpose of using masks is to prevent inhalation and to trap airborne particles (natural or man-made), and biological organisms (bacteria, viruses, prions, and fungi) (Steve Zhou *et al.*, 2018). Airborne particles of natural origin (volcanic eruptions, dust storms, naturally occurring fires) and man-made (such as industrial emissions) are on a nanometer scale. Several studies have

Figure 1.1. Representation of basic cloth mask

shown the severe impact of the respiration of nanoparticles on respiratory and cardiovascular diseases. Also, inhalation of these particles (particles smaller than 2.5 μm) resulted in an estimated 8.9 million deaths in 2015 (McDonald *et al*.,2020). Higher capacity, optimal comfort, and a high-efficiency mask for bioaerosol removal and optimal air filtration are the objectives of the studies conducted in this report. Factors affecting the determination of the final quality of the mask were focused on increasing and enhancing the effectiveness of the mask at the center of attention. In general, the filtering ability of the mask is influenced by the specifications of the mask filter and external factors. Also, studies have shown the importance of the external effect of factors such as face velocity or airflow, the steady or unsteady pattern of flow, the charge state of the particle, frequency of the respiration, relative humidity, and temperature, and loading time on the filtering efficiency of the mask (Tcharkhtchi *et al*.,2021). Because of the significant effects of external factors on the filtering performance, the determination of the filtering mechanism has a high status. It is only by clarifying and understanding these mechanisms that mask design and filtration can be enhanced and improved. There are different types of masks currently in practice. Some types of masks are discussed below.

Figure 1.2. Surgical Face mask

1.1. Types of masks

1.1.1. Face mask

These kinds of masks that cover the user's nose and mouth are used as physical barriers for the fluids and particulate materials in certain efficiency. Face masks can be classified into three categories.

Figure 1.3. Schematic of Full-length face shield

1.1.2. Basic cloth face mask

This type of mask is the simplest one that can be used during severe periods. During a pandemic respiratory because of the scarcity or availability of filtering face piece respirators, some people may prefer to use cloth products for respiratory safety. Figure 1.1 represents basic cloth masks.

1.1.3. Surgical face mask

Surgical face mask (Figure1.2) is initially designed to shield the wearer from infectious droplets in clinical environments, but it does not help much to protect from the spread of respiratory diseases While they are not an absolute method of protection, they have a shield that will protect the wearer from a stream of fluid, for example, sneezing, and capturing bacteria from the wearer's mouth and nose in liquid droplets and aerosols The commercial surgical face masks commonly had a three-layer structure. The middle layer is the filter media, whereas the inner layer is for absorbing moisture, and the outer layer repels water. However, the planar mask has a lower protection level, and it is necessary to take careful consideration of comfort sensation and protection level when choosing a planar-type mask in polluted air.

1.1.4. Full-length face shield

It is a light weighted and low-cost mask that is composed of elastic headbands through the head and a transparent rigid polymeric full-length face shield. The transparent part is made in most cases with Polycarbonate (PC). It functions as a shield to protect the face parts from the direct contact of the liquid splashes from the Infectious when speaking, sneezing, and coughing. The schematic of the full-length face shield is shown in Figure 1.3.

1.1.5. N95 respirator

These types are a type of FFR masks, are non-oil resistant, also known as electrets filters. The word N95 is obtained from the fact that these types of masks can at least filter 95% of aerosols around 0.3 μm. N95 respirator also has different types, such as surgical N95 respirator, with higher

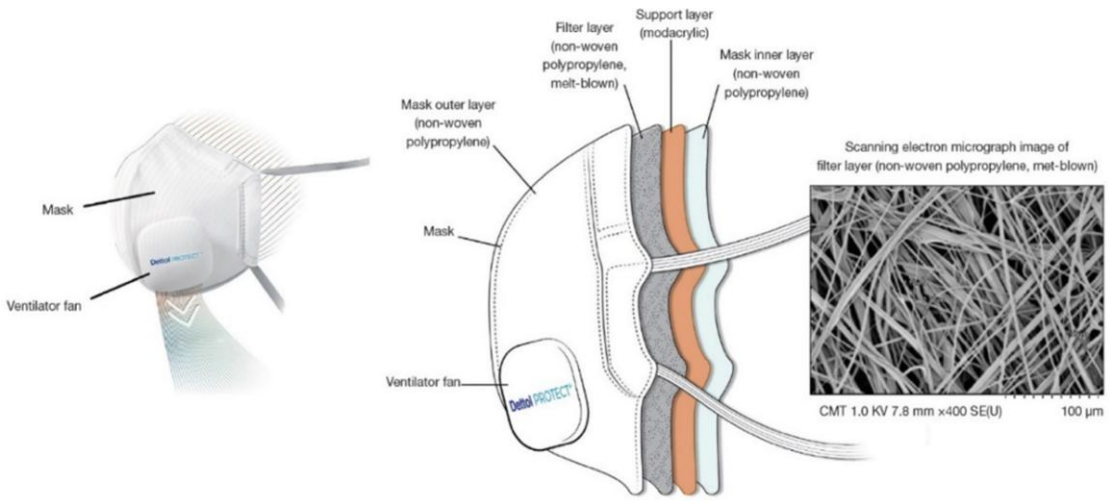

Figure 1.4. Schematic representation of the N95 mask with various layers

efficiency than the standard N95. As can be seen from Figure 1.4, the N95 respirator consists of four principal layers, which include the inner layer, support layer, filter layer, and layer mask filter layer from inside to outside of it. Also, a ventilator fan is embedded on the outer layer of N95 to improve breathing.

2. METHODS AND MATERIALS

2.1. Equipment Design

2.1.1. Mechanism of filtration

Penetration has an unprecedented dependence on the particle scale because, in the sub-micron size regime, trapping of the aerosol is occurred by different mechanisms like gravity sedimentation, inertial impaction, interception, diffusion, and electrostatic attraction. The possibility of activation of these mechanisms is examined by considering the sizes of particles. Kinetics and related mechanisms are firmly depending on the type of the active substance, consisting of the physical and chemical properties, such as molecular weight, particle size, etc.

2.1.2. Gravity sedimentation

It has been pointed out that for aerosols in the range of 1 µm – 10 µm, gravity sedimentation plays an essential role because ballistic energy or gravity forces have an early effect on the large, exhaled droplets. McCullough et al. mentioned that for the size of particles (0.5 > µm) that is expected that inertia and gravity can be the dominant mechanism, and it has been predicted that the aerosol with the smallest

size, which is polystyrene latex sphere (0.5 µm) has the most penetrating ability.

2.1.3. Inertial impaction

Inertial impact occurs when the inertia of the particles becomes too large that induces changes in the direction of particle movement in the airflow. Particles with bigger sizes, larger face velocities, and densities pose higher inertia, and this process makes them more easily captured. These particles have inertia that they are not able to flow around the respirator fibers. Moreover, instead of flowing through the filter of material, the particles with larger size stray from the air streamlines, collide with the fibers, and can adhere to them Overall, particles of around 1 µm or greater may be effectively removed by this mechanism. But it does not significantly participate in capturing mechanisms for nanoparticles. The effect of this mechanism in capturing Ultrafine particles and Nanoparticles is neglected.

It should be noted that the impact of Brownian motion on smaller particles is significant. Diffusion is commonly used as the primary aggregation mechanism for particles lower than 0.2 µm, and the particles greater than 0.2 µm are governed by detection and inertial impaction.

2.1.4. Interception

Interception happens as a particle follows the primary streamline to allow interaction between particle and filter media within one particle width of the surface of the fiber. This method is successful in extracting particles up to 0.6 µm. Interception is not explicitly determined by particle velocity, but it is more apparent as particle size decreases. There is a crucial distinction between interception and inertial impaction that there is no divergence from the central streamline for an interception, where the filter substance intercepts the particle. It has been reported that by reducing aerosol size in the interval 100 nm to 1 µm, diffusion by Brownian motion and mechanical interception of particles by the filter fibers are prevailing mechanisms.

2.1.5. Diffusion

Based on the random Brownian motion of particles bouncing into the filter media, it is the most effective mechanism for capturing particles with sizes less than 0.2 µm. Indeed, the abnormal motion of particles raises the probability of collision between particles and fiber in a streamline that does not intercept. This makes the diffusion of enormously tiny objects, such

as ultrafine particles and nanoparticles, more important than interception. As particle size or facial velocity reduces, the rate of diffusion becomes more noticeable. With lower speeds, the particle residence period is increased using filter media; hence the likelihood of collision between particle and filter media is increased dramatically. Different investigations represented that when the bulk of the outflow entered the matrix of the mask, its velocity decreased immediately because of diffusion into the mask.

For the mechanism of the mass transport, there is a general model of Fick's first law which is corresponding to the mass diffusion across a unit area in the unit of a time, and Fick's second law which indicates the change in the concentration with time in the defined region.

$$J = -D\frac{dc}{dx} \quad (1)$$

$$\frac{dc}{dt} = D\frac{d^2c}{dx^2} \quad (2)$$

Where "J" is the diffusion flux, "D" is the diffusion coefficient in dimensions, "C" is the concentration in dimensions, "x" is the position, "t" is the time.

2.1.6. Electrostatic attraction and thermal rebound

Electrostatic attraction is a method that is captured both large and small particles from the airstream. In this method, electrically charged fibers or granules are considered in the filter to absorb oppositely charged particles from the airstream. In the case of the nanometer scale, particles can slip between the openings in the network of filter fibers; removing of low mass particles has been done by electrostatic attraction, and electrostatic filters can be useful at low velocity like respiratory velocity through a facemask.

2.1.7. Penetration Measurement

The particle penetration is defined as the ratio of two concentration distributions:

$$P\% = \frac{\left(\frac{dC}{dlogD_p}\right)}{\left(\frac{dc}{dlogD_p}\right)} \quad (3)$$

C and Dp indicate the number concentration and the particle diameter, respectively; thus the term (dC/dlogDp) represents the number concentration distribution in terms of particle size (#/cm3). Subscripts d and u indicate the

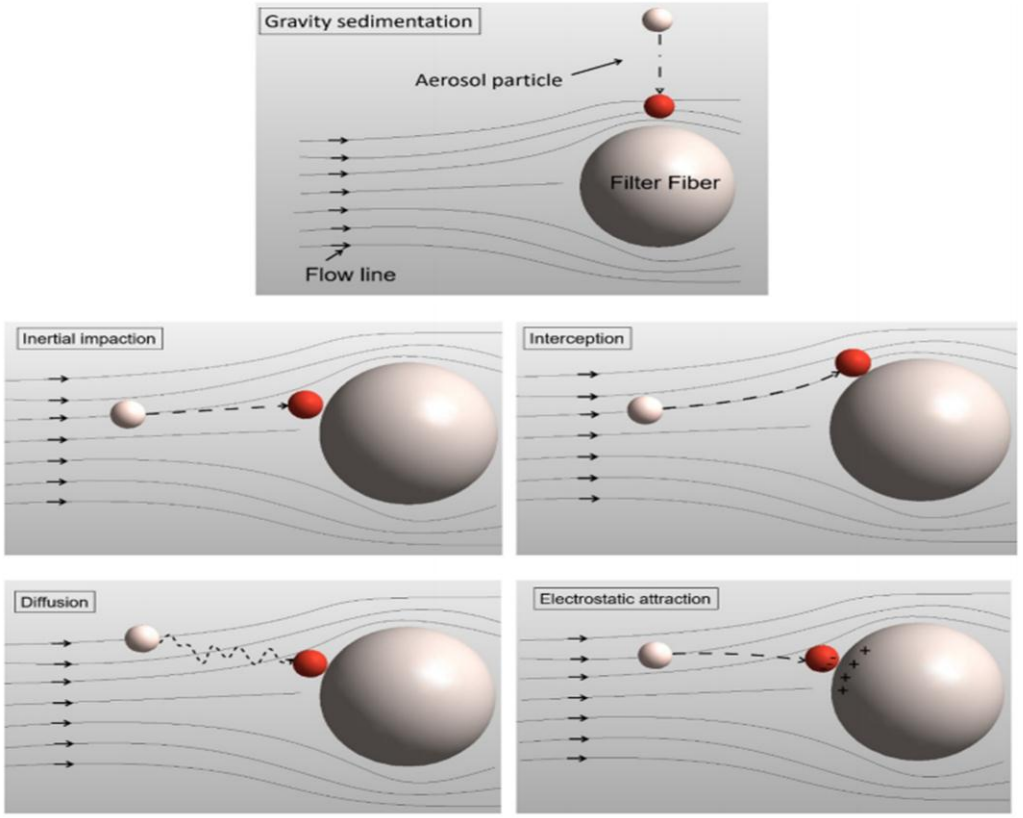

Figure 2.1. Schematic of the mechanisms of aerosol penetration through the masks

filter downstream and upstream, respectively.

2.1.8. Equations for performance evaluations of mask filters

A fibrous filter is comprised of many randomly oriented fibers which are arranged in such a way that they restrict the penetration of aerosols and prevent the flow of contaminants through the mouth and nose of the wearer. These fibers form a dense material or mat which captures and retains particles throughout their depth or thickness. Different mechanisms are needed for a mask to capture the particles and clean the filtrate. The thickness, fiber diameter, and density of the mat are critical in designing the proper face mask which affects the mask's performance.

The important parameters that determine the performance of the face masks and respirators are porosity, pressure drop, collection efficiency, and flow velocity. Porosity is the volume fraction of air contained in the fabric filter that can be expressed as:

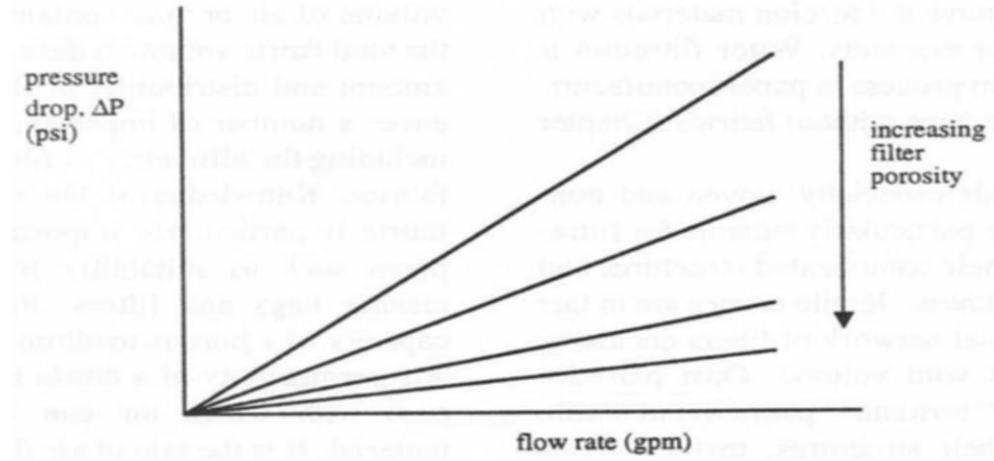

Figure 2.2. Relationship between flow rate and pressure drop for different pore size

$$Porosity = \frac{Volume\ of\ voids}{Total\ fabaric\ volume} \quad (4)$$

It is necessary to measure the airflow through the fabric, called air permeability, to construct the fabric filter to perform as desired. This is air permeability is an estimation of how much fluid can be transmitted through open space between the fibers in a fabric. It is the rate of airflow under a certain pressure differential across an area of the filter fabric. Filter performance increases as the pore size decreases; however, more back pressure can be required to achieve the same flow rate through the filter. This effect is shown in Fig.2.2.

Darcy's law describes the pressure drop across porous media as a function of flow rate and is valid for small pressure differentials. According to Darcy's Law, the relationship between the fluid flow rate and pressure drop across the porous media is linear.

$$Q = \frac{kA(P_1 - P_2)}{\mu L} \quad (5)$$

where,(P1−P2) (or ΔP) is the pressure drop of a fluid with viscosity μ, flowing at a volumetric flow rate Q over a bed of porous media of a given thickness L, cross-sectional area A and permeability k. P1 and P2 represent the pressures at high-side and low-side pressures, respectively. At higher velocities, this law becomes invalid and hence Reynold's number is used to characterize the deviation point of Darcy's law. Reynold's number, Re, is defined as the ratio of fluid density ρ,

particle diameter dp, and fluid velocity V, to the fluid viscosity μ:

$$Re = \frac{\rho d_p V}{\mu} \qquad (6)$$

It follows from equations (5) and (6) that pressure drop is proportional to the filter thickness and inversely proportional to the cross-sectional area. Pressure drop is also proportional to the face velocity because the flow in a filter is usually laminar.

The collection efficiency, E, is defined as the ratio of the number of particles stopped by the filter to the number of particles passing through the projected area of the fibrous filter.

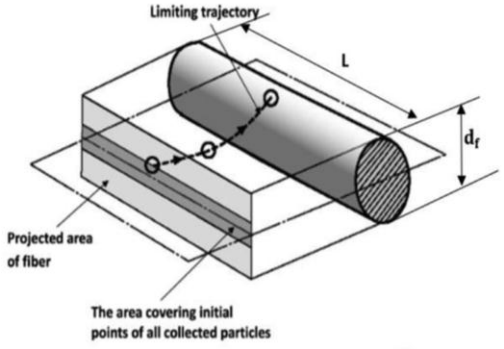

Figure 2.3. The trajectory of a particle while entering the filter

$$E = \frac{N_0 - N}{N_0} \qquad (7)$$

N_0 and N are the particles' number concentration at the inlet and outlet, respectively.

The packing density or solidity α is the volume fraction of fibers in a filter. It is an important parameter to be considered which influences the performance of a filter. Generally, the values of α range between 0.01 and 0.3. The flow velocity in a filter, V, is given by

$$V = \frac{V_0}{1 - \alpha} \qquad (8)$$

V_0 is the flow velocity at the filter face.

The overall filter efficiency can be calculated based on the single fiber efficiency and other parameters as well:

$$E = 1 - exp\left[\frac{-4\alpha\eta L}{\pi d_f (1 - \alpha)}\right] \qquad (9)$$

η is the single fiber efficiency, L is the filter thickness, and df is the fiber diameter.

2.2. Sample Materials

A total of 48 different sample materials were investigated:

- twelve pure cotton fabrics, including woven textiles with different thread counts as well as jersey and velvet cotton,
- five fabrics containing cotton mixed with synthetics, including flannel, French terry, and velour,
- eleven synthetic fiber samples including woven and jersey materials,
- four paper-like materials (paper towels, coffee filter, paper tissue),
- four natural fiber materials (linen, wool, silk),
- eight synthetic household materials such as vacuum cleaner bags, a vacuum cleaner bag backup filter, anti-allergic mattress, and linen encasements, and polyurethane (PU) foams,
- three commercially available surgical masks (EN 14683) and one FFP2 mask (EN 149); a separate surgical mask (EN 14683) was used for the measurements of the influence of leaks on filtration efficiency.

The most studied materials in fabricating masks include non-woven fibrous substances such as polypropylene, glass papers, woolen felt. These materials have been used in manufacturing personal protection equipment (PPE) since the beginning of the 20th century. These materials have proven to be capable of withstanding high temperatures during autoclaving without any changes in the structure. Masks are fabricated via melt blowing technique, during which the charges are imparted to the material creating a quasi-permanent electric field providing an adequate filtration of particulate matters (PM) by electrostatic force. The filtration efficiency of the membrane depends upon the structure (pore size, fiber organizations), the charge of the fibers, fiber thickness, and diameter, packing density, etc., of the material. It has been concluded that fibers with a small diameter and a large surface area that forms small voids when compared to long fibers, lead to increased filtering efficiency.

Several studies have been conducted to theoretically explain the process of filtration through electrostatic attraction and impaction by the fibrous medium. An early study concluded that electret filters

(non-woven fibers) hold high filtration efficiency with low air resistance and large dust holding capacity when compared to conventional fibrous filters. The filtration works based on electrostatic forces of attraction between the masks matrix and the aerosol particles and depends on the dielectric property of the material. Hence, polymeric materials with high electrical resistance and stability, such as polypropylene (PP), polyethylene, polyacrylonitrile (PAN), etc., are the best choices for masks and respirators. However, the hydrophilicity of these polymer surfaces is needed to be improved for effective trapping and filtration of aqueous particles

There are three major layers in a mask which include i) spun-bond PP fabric, ii) interlayer with melt-blown PP, and iii) external layer with spun bond PP fabric like layer (i). The middle layer comprises small voids compared to the other two layers and it acts as the filter, stopping the harmful particles from entering the body. A recent study compared three masks with

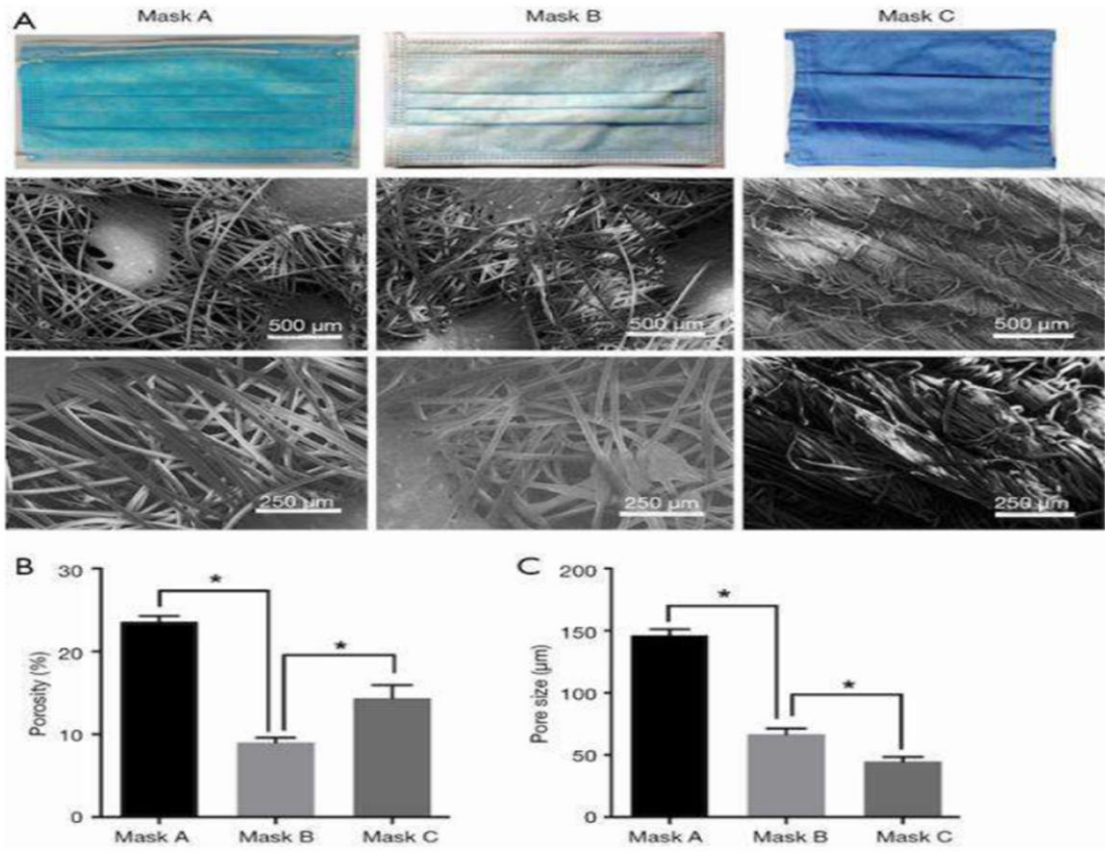

Figure 2.4. SEM images showing the fiber structure of different masks. (B) Mask porosity. (C) Mask void size distribution.

different filtration efficiency, porosity, and airflow resistance, Mask A with one filter screen, Mask B with two filters, and a washable cloth Mask C. It was concluded that Mask B provided the best filtration owing to its lowest porosity and highest filtering efficiency. Mask A possessed large voids, leading into reduced filtration efficiency whereas Mask C had the highest airflow resistance, leading to breathing difficulties (Fig.2.4).

2.2.1. Recent Advances

Recently, several studies have been performed to improve the efficiency of the respirators and masks against ultra-fine particles such as viruses and other pathogens. These include employing modified filter materials such as nanofibres and nanofibre webs. Also, the virus disinfection capability can be improved by treating the filter surfaces with materials that possess antimicrobial properties. The use of silver nanoparticles (AgNPs), copper oxide, iodine, titanium oxide (TiO2), etc, have already been reported in the past decades. With the rapid growth of nanotechnology, the fabrication and development of nanomaterials have been improved significantly.

The use of nanofibres in masks and respirators has increased widely since the last decade. Nano-sized fibers offer a very high surface area per unit mass that can improve the capture efficiency as well as other surface areas dependent phenomena such as ion exchange and catalysis. They have a small void size, low weight, improved permeability, and good interconnectivity of voids. Functionalizing the nanofibres with chemicals and nucleating agents also helps in decomposing or deactivating the contaminants, which will reduce the risk of inhaling pathogens and viruses. Electrospinning techniques are most commonly used for the fabrication of nanofibres. Skaria et al. demonstrated that nanofibre filter incorporated surgical masks showed a decrease in airflow resistance and an improved filtration efficiency when compared to commercially available masks. A recent study investigated the mask fit and usability of traditional N95 FFPR with the nanofibre N95 FFPR by analyzing before and after nursing procedures. It was concluded that the nanofibre FFR possessed a higher pass rate for the fit testing compared to 3M FFRs. It was also observed to possess a higher bacterial

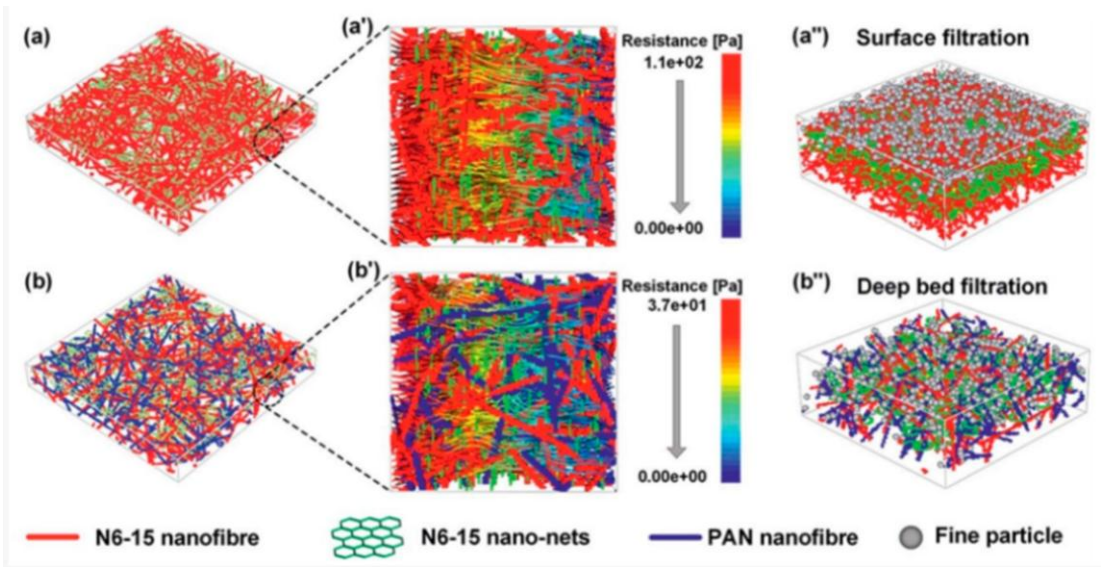

Figure 2.4. (a) 3D N6-15 NFN and (b) N6–PAN NNB geometric structures simulated with FibreGeo based on the bulk statistical properties; (a′) and (b′) is the airflow resistance distributions in the cross-sections of the relevant membranes; (a″) surface and (b″) deep bed particle loading simulations on 3D tomography images.

filtration efficiency than the commercially available version in the market. The nanofibre FFPR consisted of partially gelled submicron and nanofibres of PP, and a hydrophilic biocide layer that could effectively inactivate pathogens. It was found that nanofibre FFPR demonstrated significantly better air permeability and higher antibacterial activities than normal N95 respirators and surgical masks.

The introduction of another polymer layer could create excellent filtration media and hence composting of materials in a filter media has gained much attention. Compositing another layer of filter material with the electret fibers improved the electrostatic charge retention, hence improving the overall filtration efficiency. An ultra-lightweight binary structure of nylon 6-polyacrylonitrile nanofibre net (N6-PAN NNB) was fabricated by Wang et al. for the enhanced capture of fine particles with a diameter of 2.5 μm or less (PM 2.5) N6-PAN NNB was synthesized from nanofibres of polyacrylonitrile (PAN) and polyamide 6-15 (PA6-15) through multi-jet spinning. The composite showed 99.99% filtration efficiency when compared to the commercial fibers available and offered a deep bed filtration pattern in contrast to the surface filtration pattern of normal fibers. A 3D simulation of the structure was also formulated and an

airflow resistance model was developed based on the experimental data observed. A very recent study reported the fabrication of a nanofibre composite of PP nanofibres coated with cellulose acetate (CA) and polyvinylidene fluoride (PVDF) to meet the requirements of N95 respirators.

3. COST ESTIMATION CALCULATION

- Twelve pure cotton fabrics, including woven textiles with different thread counts as well as jersey and velvet cotton = 0.25*12=3
- Five fabrics containing cotton mixed with synthetics, including flannel, French terry, and velour = 5*0.25=1.25
- Eleven synthetic fiber samples including woven and jersey materials= 11*0.25=2.75
- Four paper-like materials (paper towels, coffee filter, paper tissue)= 4*0.25=1
- Four natural fiber materials (linen, wool, silk)= 4*0.5=2

Total Cost =3+1.25+2.75+1+2= $10.

4. CONCLUSION

Different mechanisms were influential in the penetration of the particles through the masks. Some environmental parameters are playing a significant role in the attributed mechanism and, in consequence, the filtration efficiency. Thus, the choice of the mask also depends on the environmental condition of the usage. Among all the affecting parameters, the particle size and flow rate have resulted as the most important ones. The property referred to as the quality fabrication of the masks is important. Where increasing the thickness and numbers of the layers, packing density, fiber charge density, and decreasing fiber diameter, increase the filtering efficiency.

Considering the advantages, disadvantages, and capabilities of the different kinds of masks, it seems that there is much to do in this field to propose a special kind of mask for a certain issue, whereby increasing the filtration efficiency, comfortability and accessibility decreases among the people Nevertheless, it is comprehensible that referring to the different types of climate conditions, diverse physiological state of humans, etc., one type of mask may not be universal for a certain issue. The total estimated cost for the production of single fibrous filter bed masks is $10.

5. ACKNOWLEDGEMENT

NA.

6. CONFLICT OF INTEREST

The author declares no conflicts of interest.

7. SOURCE(S) OF FUNDING

The author did not require funding.

8. REFERENCES

1. McDonald, Fiona, et al. 2020. "Facemask Use for Community Protection from Air Pollution Disasters: An Ethical Overview and Framework to Guide Agency Decision Making." *International Journal of Disaster Risk Reduction* 43(June 2019): 101376. https://doi.org/10.1016/j.ijdrr.2019.101376.
2. Steve Zhou, S., Lukula, S., Chiossone, C., Nims, R. W., Suchmann, D. B., & Ijaz, M. K. (2018). Assessment of a respiratory face mask for capturing air pollutants and pathogens including human influenza and rhinoviruses. *Journal of Thoracic Disease*, *10*(3), 2059–2069. https://doi.org/10.21037/jtd.2018.03.103
3. GBD 2015 Risk Factors Collaborators, Global, regional, and national comparative risk assessment of 79 behavioural, environmental and occupational, and metabolic risks or clusters of risks, 1990-2015: a systematic analysis for the Global Burden of Disease Study 2015, The Lancet 388 (10053) (2016) 1659–1724, https://doi.org/ 10.1016/S0140-6736(16)31679-8.
4. R. Burnett, H. Chen, M. Szyszkowicz, N. Fann, B. Hubbell, C.A. Pope, J.V. Spadaro, Global estimates of mortality associated with long-term exposure to outdoor fine particulate matter, Proc. Natl. Acad. Sci. 115 (38) (2018) 9592–9597, https://doi.org/10.1073/pnas.1803222115.
5. D.E. Schraufnagel, J.R. Balmes, C.T. Cowl, S. De Matteis, S.-H. Jung, K. Mortimer, D.J. Wuebbles, Air pollution and noncommunicable diseases: a review by the forum of international respiratory societies' environmental committee, Part 1: the damaging effects of air pollution, Chest 155 (2) (2019) 409–416, https://doi.org/ 10.1016/j.chest.2018.10.042.

6. World Health Organization. Burden of disease from the joint effects of Household and Ambient Air Pollution for 2012. WHO Technical Report. Available online: HTTP:// www.who.int/phe/health_topics/outdoor-air/databases/AP_ jointeffect_BoD_results_March2014.pdf
7. Pope CA 3rd, Burnett RT, Thun MJ, et al. Lung cancer, cardiopulmonary mortality, and long-term exposure to fine particulate air pollution. JAMA 2002;287:1132-41.
8. Hoek G, Krishnan RM, Beelen R, et al. Long-term air pollution exposure and cardio-respiratory mortality: a review. Environ Health 2013;12:43.
9. Yang G, Wang Y, Zeng Y, et al. Rapid health transition in China, 1990-2010: findings from the Global Burden of Disease Study 2010. Lancet 2013;381:1987-2015.
10. Zhang X, Li H, Shen S, et al. An Improved FFR Design with a Ventilation Fan: CFD Simulation and Validation. PLoS One 2016;11:e0159848.
11. Wei J, Li Y. Airborne spread of infectious agents in the indoor environment. Am J Infect Control 2016;44:S102-8
12. Rohde RA, Muller RA. Air Pollution in China: Mapping of Concentrations and Sources. PLoS One 2015;10:e0135749.
13. Borkow G, Zhou SS, Page T, et al. A novel anti-influenza copper oxide containing respiratory face mask. PLoS One 2010;5:e11295.
14. Finney DJ. Statistical methods in a biological assay. 3rd edition. New York: McMillan Co., Inc., 1978:394-401.

World Climate Congress 2021
International Journal of Applied Chemical and Biological Sciences
ISSN: 2582-788X

DESIGN OF CONVENTIONAL CYCLONE BY SHEPHERD AND LAPPEL MODEL

Awanish Adhikari, Dinesh Joshi *, Ojash Giri

Department of Environmental Science and Engineering, Kathmandu University, Dhulikhel, Nepal

* For correspondence: joshidinesh0227@gmail.com

Abstract

This study has developed theoretical methods for computing travel distance, numbers of turns and cyclone pressure drop in order to estimate the cyclone performance which is a must if any one wishes to design a cyclone abatement system for particulate control. The flow pattern and cyclone dimensions determine the travel distance in a cyclone. The number of turns was calculated based on this travel distance. The new theoretical analysis of cyclone pressure drop was tested against measured data at different inlet velocities and gave excellent agreement. The results show that cyclone pressure drop varies with the inlet velocity, but not with cyclone diameter. Cyclone cut-points for different dusts were traced from measured cyclone overall collection efficiencies and the theoretical model for calculating cyclone overall efficiency. The cut-point correction models 2D cyclones were developed through regression fit from traced and theoretical cut-points Diameter. Experimental results indicate that optimal cyclone design velocities, which are for 2D cyclones, should be determined based on standard air density. It is important to consider the air density effect on cyclone performance in the design of cyclone abatement systems. The tangential inlet generates the swirling motion of the gas stream, which forces particles toward the outer wall where they spiral in the downward direction. Eventually the particles are collected in the dustbin located at the bottom of the conical section of the cyclone body. The cleaned gas leaves through the exit pipe at the top.

Keywords: cyclone separator, particulate control

1. INTRODUCTION

With the beginning of industrialization human group transform from agrarian society into an industrial society. Industrialization came to be a boon to human society in terms of ease of work load and variety of services that has been offered by the development of new technologies each year continuously. But every boon has some curse associated with it. The development of industrialization brought ease of life to human beings but it came with a price that the environment has to pay. The disadvantage of industries is that it releases some kind or other type of pollution to the environment which is directly or indirectly harmful to human beings, other animals, plant and vegetation. Every aspect of the environment including land, water, air and soil has been polluted. Engineers have been coming up with many technologies that counter balances such pollution emitted to environment.

One of such pollution emitted to environmental by different industries is particulate matter. Particulate matter are microscopic particles of solid or liquid matter suspended in the air. They have impacts on climate and precipitation that adversely affect human health, in ways additional to direct inhalation. Man-made activities such as fuel combustion, industrial processes, steel industry, petroleum foundries, cement, glass manufacturing industry, smelting and mining operations, fly-ash emissions from power plant, burning of coal, and agricultural refuse also contribute to PM in the atmosphere. Appropriate techniques can be used to separate such particulate matter from the stream of exhaust air that is to be released to the environment. The separation processes include Gas-Liquid (vapor-liquid) separation, Gas-Solid separation (vapor-solid), Liquid-Liquid separation (immiscible), Liquid Solid, and Solid-Solid separation etc. Gravitational force or centrifugal force can be used to enhance the separation. The main techniques used to separate the phases, and the components within the phases, are discussed in details. The principle methods for the separation of such mixtures could be classified as:

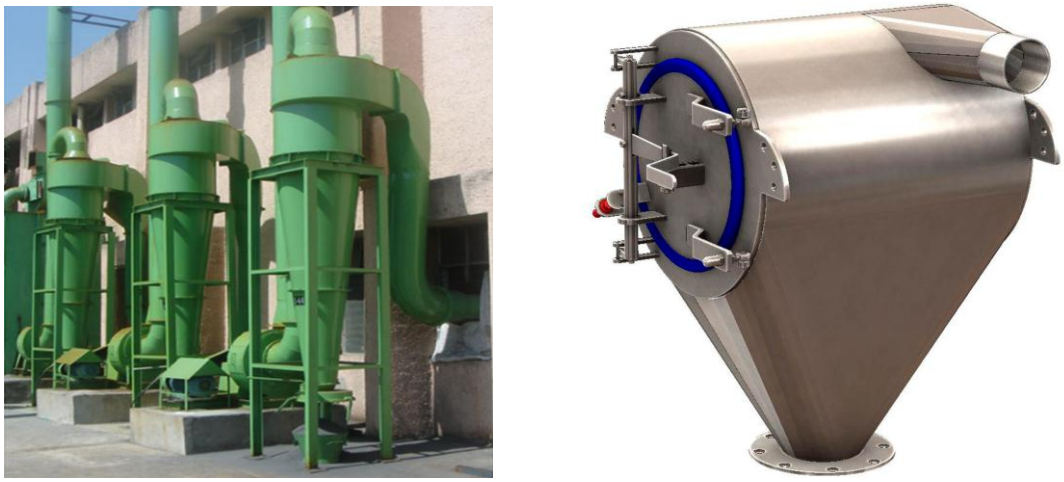

Figure 1. Cyclone Seperator

1. Cyclone separator, 2. Gas-Liquid separator, 3. Liquid-Liquid separator, 4. Gravity separator, 5. Centrifugal separator, 6. High speed tubular centrifuge, 7. Scrubbers, 8. Electrostatic precipitator, 9. Hydro cyclone.

1.1. Cyclone Separator

Cyclone separators provide a method of removing particulate matter from air or other gas streams at low cost and low maintenance. Cyclones are somewhat more complicated in design than simple gravity settling systems, and their removal efficiency is much better than that of settling chamber. Cyclones are basically centrifugal separators, consists of an upper cylindrical part referred to as the barrel and a lower conical part referred to as cone (figure 5.1). They simply transform the inertia force of gas particle flows to a centrifugal force by means of a vortex generated in the cyclone body. The particle laden air stream enters tangentially at the top of the barrel and travels downward into the cone forming an outer vortex. The increasing air velocity in the outer vortex results in a centrifugal force on the particles separating them from the air stream. When the air reaches the bottom of the cone, it begins to flow radially inwards and out the top as clean air/gas while the particulates fall into the dust collection chamber attached to the bottom of the cyclone.

1.2. Types of Cyclone

Three different types of cyclone are shown in figure 2. First figure i.e. 2a shows a cyclone with a tangential entry. These

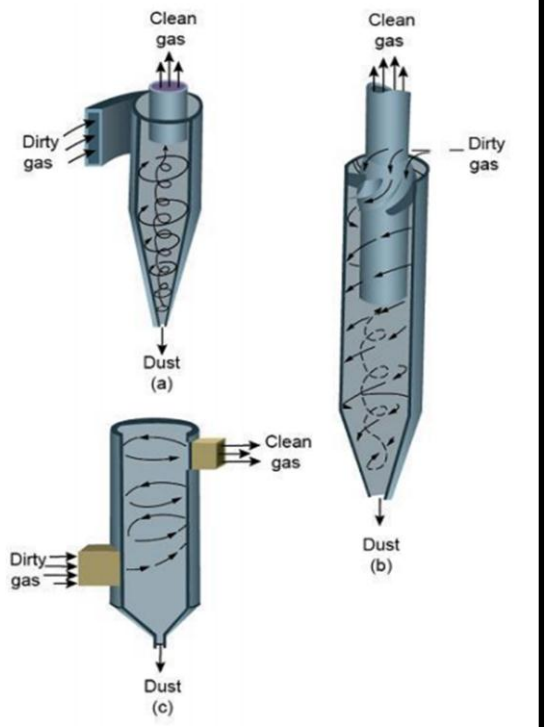

Figure 2. Types of cyclone separator

types of cyclones have a distinctive and easily recognized form and widely used in power and cement plants, feed mills and many other process industries. Figure 2b shows the axial entry cyclones, the gas enter parallel to the axis of the cyclone body. In this case the dust laden gases enter from the top and are directed into a vortex pattern by the vanes attached to the central tube. Axial entry units are commonly used in multi cyclone configuration, as these units provide higher efficiencies. Another type of larger cyclonic separator shown in figure 2c is often used after wet scrubbers to trap particulate matter entrained in water droplets. In this type, the air enters tangentially at the bottom, forming vertex. Large water droplets are forced against the walls and are removed the air stream. Cyclone collectors can be designed for many applications, and they are typically categorized as high efficiency, conventional (medium efficiency), or high throughput (low efficiency). High efficiency cyclones are likely to have the highest-pressure drops of the three cyclone types, while high throughput cyclones are designed to treat large volumes of gas with a low pressure drop. Each of these three cyclone types has the same basic design. Different levels of collection efficiency

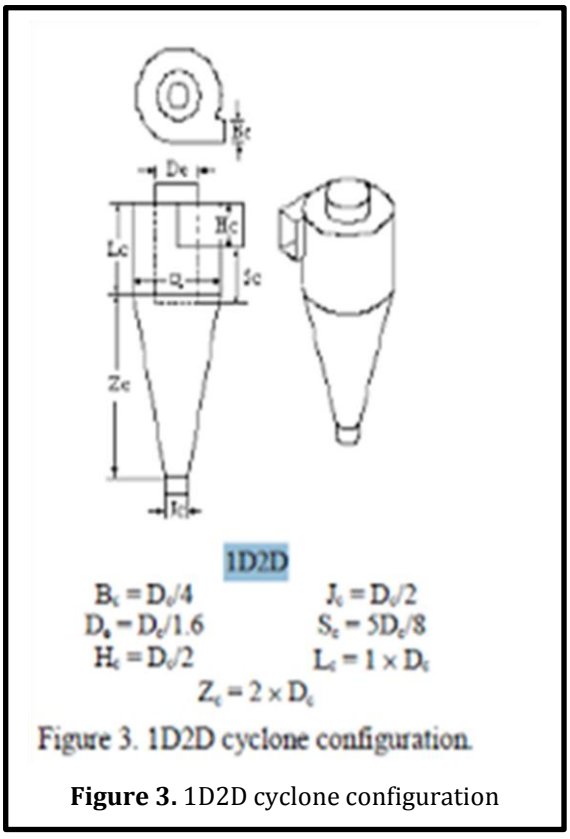

Figure 3. 1D2D cyclone configuration.

Figure 3. 1D2D cyclone configuration

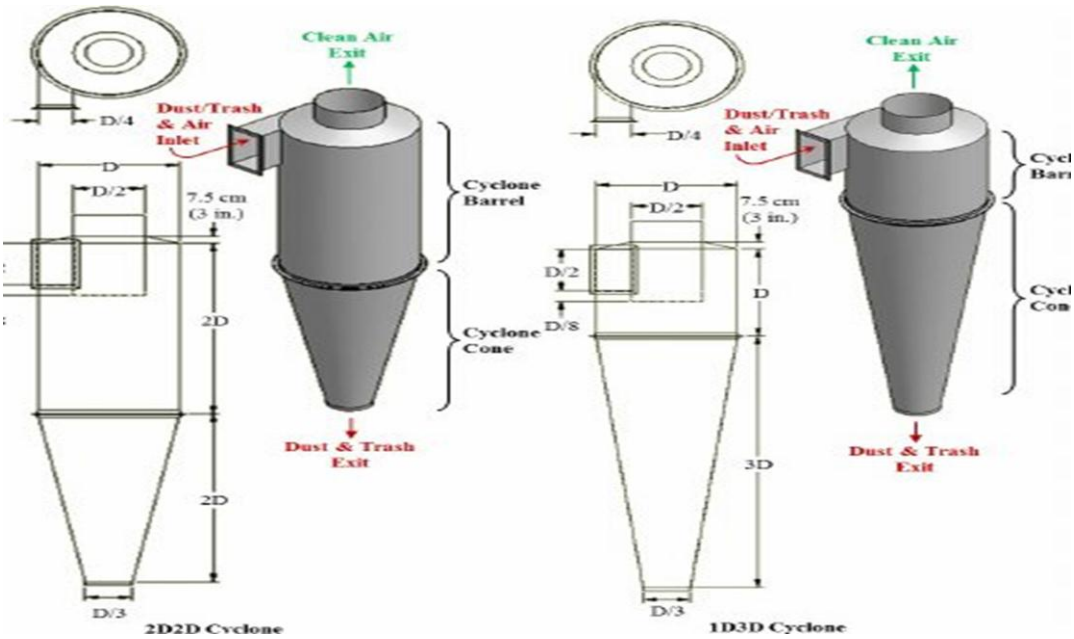

Figure 4. 2D2D cyclone and 1D3D cyclone

and operation are achieved by varying the standard cyclone dimensions.

1.3. Different Cyclone Model

In the agricultural processing industry, 2D2D (Shepherd and Lapple, 1939) and 1D3D (Parnell and Davis, 1979) cyclone designs are the most commonly used abatement devices for particulate matter control. The D's in the 2D2D designation refer to the barrel diameter of the cyclone. The numbers preceding the D's relate to the length of the barrel and cone sections, respectively. A 2D2D cyclone has barrel and cone lengths of two times the barrel diameter, whereas the 1D3D cyclone has a barrel length equal to the barrel diameter and a cone length of three times the barrel diameter. The configurations of these two cyclone designs are shown in figure 2. Previous research (Wang, 2000) indicated that, compared to other cyclone designs, 1D3D and 2D2D are the most efficient cyclone collectors for fine dust (particle diameters less than 100 µm). Mihalski et al (1993) reported "cycling lint" near the trash exit for the 1D3D and 2D2D cyclone designs when the PM in the inlet air stream contained lint fiber. Mihalski reported as significant increase in the exit PM concentration for these high efficiency cyclone designs and attributed this to small balls of lint fiber "cycling" near the trash exit causing the fine PM that would normally be collected to be diverted to the clean air exit stream. Simpson and

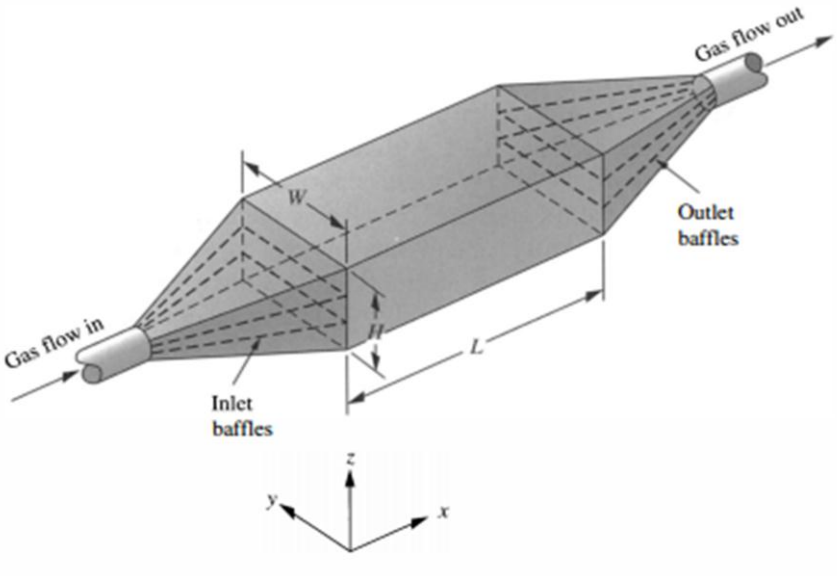

Figure 5. Gravity settler

Parnell (1995) introduced a new low-pressure cyclone, called the 1D2D cyclone, for the cotton ginning industry to solve the cycling-lint problem. The 1D2D cyclone is a better design for high-lint content trash compared with 1D3D and 2D2D cyclones (Wang et al., 1999). Figure 3 illustrates the configuration of 1D2D cyclone design.

Similarly, cyclone efficiency will decrease with increases in the parameters such as gas viscosity; cyclone body diameter; gas exit diameter; gas inlet duct area; gas density; leakage of air into the dust outlet. The efficiency of a cyclone collector is related to the pressure drop across the collector. This is an indirect measure of the energy required to move the gas through the system. The pressure drop is a function of the inlet velocity and cyclone diameter. Form the above discussion it is clear that small cyclones are more efficient than large cyclones. Small cyclones, however, have a higher pressure drop and are limited with respect to volumetric flow rates. Another option is arrange smaller cyclones in series and/or in parallel to substantially increase efficiency at lower pressure drops. These gains are somewhat compensated, however, by the increased cost and maintenance problems. Also these types of arrangements tend to plug more easily. When common hoppers are used in such arrangements, different flows through cyclones can lead to re-entrainment problems. A typical series arrangement is

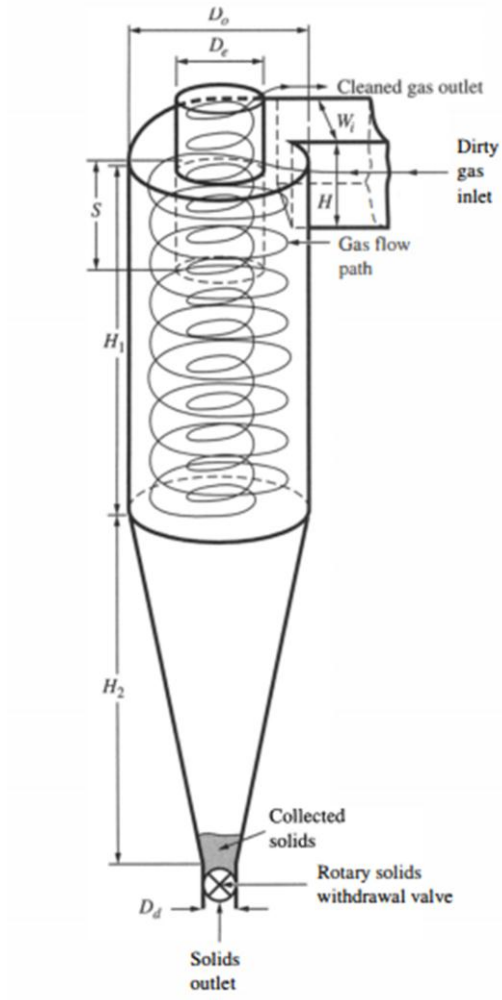

Figure 6. A Conventional cyclone

shown in figure In such arrangements large particle can be arrested in the first cyclone and a smaller, more efficient cyclone can collect smaller particles. Due to that it reduces dust loading in the second cyclone and avoids problems of abrasion and plugging. Also, if the first cyclone is plugged, still there will be some collection occurring in the second cyclone. The additional pressure drop produced by the second cyclone adds to the overall pressure drop of the system and higher pressure can be a disadvantage in such series system design. Cyclone efficiency can also be improved if a portion of the flue gas is drawn through the hopper. An additional vane or lower pressure duct can provide this flow. However, it may then become necessary to recirculate or otherwise treat this as purge exhaust to remove uncollected particulate matter.

2. PROCESS DESIGN

2.1. Main principles

For the design calculation purpose of a cyclone, the main force responsible for the settling of particulate matter is centrifugal force. Gravity settler use gravity for settling the particle which has a lower separation efficiency when compared with a cyclone as centrifugal force is much greater than the gravity force, The centrifugal force is normally more than 100 times the gravitational force.

If a body moves in a circular path with radius r and velocity Vc along the path, then it has angular velocity $\omega = V_c/r$, and

Centrifugal force $= mV^2_c/r = m\omega^2 r$ (1)

The forces acting on a spherical particle settling through a fluid under the influence

of gravity is given by Newtin's law for the particle,

$ma = p_{part}(\pi/6)D^3g - p_{fluid}(\pi/6)D^3g - F_d$(2)

The rna term represents the sum of the forces acting on the particle, equal to the downward acceleration of the particle. The three terms on the right represent, respectively, the gravity, buoyant, and drag forces acting on the particle. As we shall see later (and all know from personal experience), these drag (or air resistance) forces increase with increasing speed and are zero for zero speed. If the particle starts from rest, its initial velocity is zero, so the drag force in this equation is initially zero. The particle accelerates rapidly; as it accelerates, the drag force increases as the velocity increases, until it equals the gravity force minus the buoyant force. At this terminal settling velocity, the sum of the forces acting is zero, so the particle continues to move at a constant velocity. To find this velocity, we set the acceleration to zero in Eq. (2) and find

$F_d = (\pi/6)D^3g(p_{part} - p_{fluid}$ (3)

To find the velocity, we need the relation between Fd and the velocity. Stokes worked this out mathematically for a set of assumptions, finding

$F_d = 3\pi\mu DV$ (4)

where μ= the viscosity of the fluid. If we substitute Eq. 4 into Eq. 3 and solve for V, we find

$V = gD^2 (p_{part} - p_{fluid})/18\mu$ (5)

which is commonly referred to as Stokes' law.

To obtain the centrifugal equivalent, we substitute the centrifugal force for the gravitational force (or the centrifugal acceleration for the gravitational acceleration, since masses are equal. And we drop the buoyant term because for the particle in gases this term is too small. In Eqs. (3) and (5) we replace g by V2c/r or byω2r. Doing this poses a problem, because now there are two velocities in the equation that are not the same. To save confusion we will call the terminal settling velocity in the radial direction Vt and the velocity along the circular path Vc.

Now substituting this centrifugal acceleration for the gravitational one in Eq.5 and dropping the pfluid term, we find

$V_t = V_c^2D^2p_{part}/(18\mu r)$ (6)

The cyclone separator is merely a gravity settler that has been made in the form of two concentric helices. Only the outer

helix contributes to collection; particles that get into the inner helix, which flows upward to the gas outlet, escape uncollected. Thus the outer helix is equivalent to the gravity settler. To find the calculation for the cyclone we will first study the behavior of a gravity settler.

Figure 5 shows a gravity settler. Its cross-sectional area (WH) is much larger than that of the duct approaching it or leading the gas away from it, so that the gas velocity inside is much lower than in either of those two ducts. Baffles of some kind are used to spread the incoming flow evenly across the settling chamber; without baffles most of the flow will go through the middle and poor particle collection will result. To calculate the behavior of such a device, chemical engineers generally rely on one of two models. Either we assume that the fluid going through is totally unmixed (block flow or plug flow model) or we assume total mixing, either in the entire device or in the entire cross section perpendicular to the flow (backmixed or mixed model). Each of these sets of assumptions leads to simple calculations. The observed behavior of nature most often falls between these two simple cases, so that with these two models we can set limits on what nature probably does. Both models are widely used in air pollution control device calculations. We will calculate the behavior of a gravity settler for block flow.

For the block flow the average horizontal gas velocity in the chamber is

$V_{avg} = Q/(WH)$ (7)

For the block flow model, we will assume

1. The horizontal velocity of the gas in the chamber is equal to Vavg everywhere in the chamber.
2. The horizontal component of the velocity of the particles in the gas is always equal to Vavg.
3. The vertical component of the velocity of the particles is equal to their terminal settling velocity due to gravity, VI'.
4. If a particle settles to the floor, it stays there and is not re-entrained.

With these assumptions we can compute the behaviour of a gravity settling chamber according to the block flow model.

$t = L/(V_{avg})$ (8)

During that time the particle will settle by a gravity a distance,

Vertical settling distance = $t\ V_t = V_t\ L/V_{av}$ (9)

If this distance is greater than or equal to h (its original distance above the floor), then it will reach the floor of the chamber and be captured. If all the particles are of the same size (and hence have the same value of VI), then there is some distance above the floor (at the inlet) below which all of the particles will be captured, and above which none of them will be captured. If we now further assume that all of the particles are the same size, that they are distributed uniformly across the inlet of the chamber, and that they do not interact with one another.

Fraction captured = $\eta = L\ V_t/(H\ V_{avg})$ (10)

To compute the efficiency-particle diameter relationship, we replace the terminal settling velocity in Eq. (10) with the terminal settling velocity given in Eq.5, we find

$\eta = LgD^2\rho_{part}/(HV_{avg}18\mu)$ (11)

As the sketch shows, a cyclone consists of a vertical cylindrical body, with a dust outlet at the conical bottom. The gas enters through a rectangular inlet, normally twice as high as it is wide, arranged tangentially to the circular body of the cyclone, so that the entering gas flows around the circumference of the cylindrical body, not radially inward. The gas spirals around the outer part of the cylindrical body with a downward component, then turns and spirals upward, leaving through the outlet at the top of the device. During the outer spiral of the gas the particles are driven to the wall by centrifugal force, where they collect, attach to each other, and form larger agglomerates that slide down the wall by gravity and collect in the dust hopper in the bottom.

The inlet stream has a height Wi in the radial direction, so that the maximum distance any particle must move to reach the wall is Wi (defined on Fig. 6). The comparable distance in a gravity settler is H (Fig. 5). The length of the flow path is $N\pi Do$, where N is the number of turns that the gas makes traversing the outer helix of the cyclone, before it enters the inner helix, and Do is the outer diameter of the cyclone. This length of the flow path corresponds to L in the gravity settler. Making these substitutions directly into the gravity settler efficiency equations, Eqs. (11),

We find: $\eta = \pi NV_cD^2\rho_{part}/(9W_i\mu)$ (12)

Here D is the particle diameter. The outside diameter of the cyclone, Do, does

not appear directly but only indirectly through Wi, which is proportional to it.

2.2. Cut Diameter

Cut diameter of a particle is a diameter for which the efficiency curve has the value of 0.50, i.e., 50 percent. We can substitute this definition into Eq. (12) and solve for the cut diameter that goes with Stokes' law, block flow model, finding:

$$D_{cut} = (9W_i\mu/(2\pi NV_c p_{part}))^{1/2} \quad (13)$$

2.3. Shepherd and Lappel Model

2.3.1. Classical Cyclone Design (CCD)

The cyclone design procedure outlined in Cooper and Alley (1994), hereafter referred to as the classical cyclone design (CCD) process, was developed by Lapple in the early 1950s. The CCD process (the Lapple model) is perceived as a standard method and has been considered by some engineers to be acceptable. However, there are several problems associated with this design procedure. First of all, the CCD process does not consider the cyclone inlet velocity in developing cyclone dimensions. It was reported (Parnell, 1996) that there is an "ideal" inlet velocity for the different cyclone designs for optimum cyclone performance. Secondly, the CCD does not predict the correct number of turns for different type cyclones. The overall efficiency predicted by the CCD process In order to use the CCD process, it is assumed that the design engineer will have knowledge of (1) flow conditions, (2) particulate matter (PM) concentrations and particle size distribution (PSD) and (3) the type of cyclone to be designed (high efficiency, conventional, or high throughput). The PSD must be in the form of mass fraction versus aerodynamic equivalent diameter of the PM. The cyclone type will provide all principle dimensions as a function of the cyclone barrel diameter (D). With these given data, the CCD process is as follows.

2.4. Standard Cyclone Dimensions

Extensive work has been done to determine in what manner dimensions of cyclones affect performance. In some classic work that is still used today, Shepherd and Lapple (1939, 1940) determined "optimal" dimensions for cyclones. Subsequent investigators reported similar work, and the so-called "standard" cyclones were born. All dimensions are related to the body diameter of the cyclone so that the results can be applied generally. The table on the

Table 1. Standard cyclone dimensions

	Cyclone Type					
	High Efficiency		Conventional		High Throughput	
	(1)	(2)	(3)	(4)	(5)	(6)
Body Diameter, D/D	1.0	1.0	1.0	1.0	1.0	1.0
Height of Inlet, H/D	0.5	0.44	0.5	0.5	0.75	0.8
Width of Inlet, W/D	0.2	0.21	0.25	0.25	0.375	0.35
Diameter of Gas Exit, D_e/D	0.5	0.4	0.5	0.5	0.75	0.75
Length of Vortex Finder, S/D	0.5	0.5	0.625	0.6	0.875	0.85
Length of Body, L_b/D	1.5	1.4	2.0	1.75	1.5	1.7
Length of Cone, L_c/D	2.5	2.5	2.0	2.0	2.5	2.0
Diameter of Dust Outlet, D_d/D	0.375	0.4	0.25	0.4	0.375	0.4

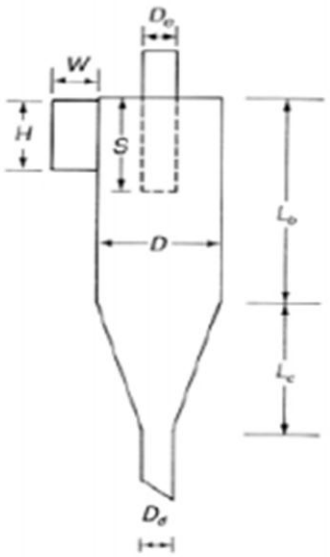

next slide summarizes the dimensions of standard cyclones of the three types mentioned in the previous figure. The side figure illustrates the various dimensions used in the table.

2.5. The Number of Effective Turns (Ne)

The first step of CCD process is to calculate the number of effective turns. The number of effective turns in a cyclone is the number of revolutions the gas spins while passing through the cyclone outer vortex. A higher number of turns of the air stream result in a higher collection efficiency. The Lapple model for Necalculation is as follows:

$N = 1/H(L_b + L_c/2)$

Where

N = number of turns inside the device (no units)

H = height of inlet duct (m or ft)

L_b = length of cyclone body (m or ft)

L_c = length (vertical) of cyclone cone (m or ft).

Based on equation the predicted numbers of turns for 4 cyclone designs were calculated. 1D2D, 2D2D, and 1D3D cyclones are the cyclone designs shown in figures 2 and 3. These three cyclone designs have the same inlet dimensions (Hc and Bc), referred to as the 2D2D inlet. The 1D3D cyclone is a traditional 1D3Dt cyclone design, which has the same design dimensions as 1D3D.

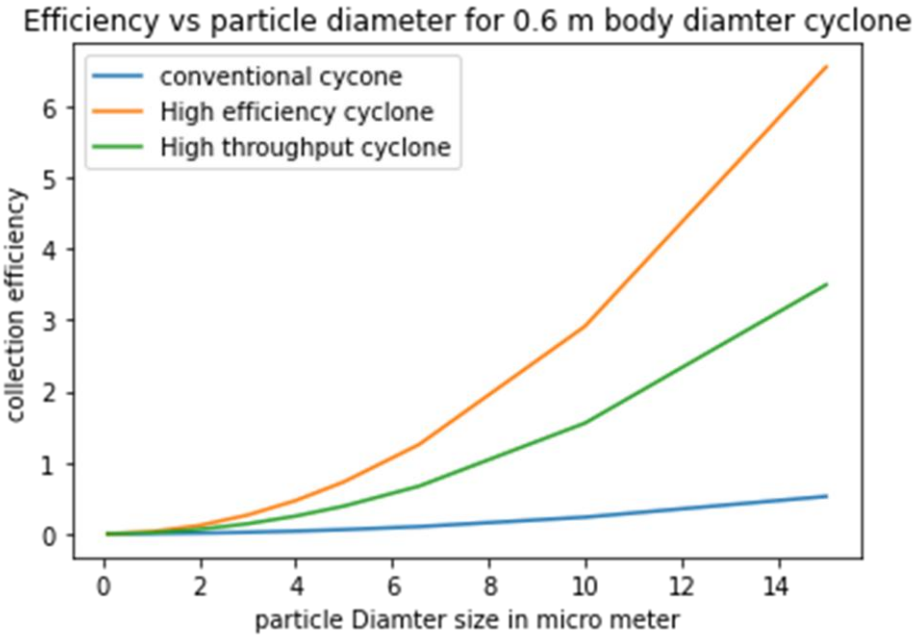

Figure 7. Collection Efficiency vs Particle Diameter

It has been observed that the Lapple model for Nproduces an excellent estimation of the number of turns for the 2D2D cyclone designs. However, this model cyclones in figure 2 except the inlet dimensions. The 1D3Dt cyclone has an inlet height equal to the barrel diameter (Hc = Dc) and an inlet width of one eighth of the barrel diameter (Bc = Dc /8). Table 1 gives the comparison of the predicted Ne vs. the observed Ne fails to give an accurate estimation of Ne for the cyclone design other than 2D2D design. This observation indicates a limitation for the Lapple model to accurately predict the number of effective turns. The Ne model is valid only for 2D2D cyclone designs, which was originally developed by Shepherd and Lapple (1939).

2.6. Gas Residence time

To be collected, particles must strike the wall within the amount of time that the gas travels in the outer vortex. The gas residence time in the outer vortex is

Δt = path length/speed = $\pi DN/V_t$

Δt = time spent by gas during spiraling descent(sec)

D = cyclone body diameter (m or ft)

Vt = gas inlet velocity (m/s or ft/s) = Q/WH

Q = volumetric inflow (m^3/s of ft^3/s)

H = height of inlet(m or ft)

W = width of inlet(m or ft)

The maximum radial distance traveled by any particle is the width of the inlet duct W. The centrifugal force quickly accelerates the particle to its terminal velocity in the outward (radial) direction, with the opposing drag force equaling the centrifugal force. The terminal velocity that will just allow a particle initially at distance W away from thewall to be collected in time is

$V_t = W/\Delta t$

Where V_t = particle drift velocity in the radial direction(m/s or ft/s).

The particle drift velocity is a function of particle size.

Assuming stokes regime flow(drag force = $3\ \pi\mu d_p V_t$) and spherical particle subjected to a centrifugal force mv^2/r with m = mass of particle in excess of air displaced, v = V_t of inlet flow and r = D/2,

we obtain,

$V_t = ((p_p - p_a)d^2_p V_t^2)/(9\mu D)$

Where,

V_t = Terminal drift transverse velocity (m/s of ft/s)

d_p = diameter of the particle (m or ft)

p_p = density of the particle(kg/m3)

p_a = air density (kg/m3)

μ = air viscosity (kg/m.s)

2.7. Fractional Efficiency Curve

The third step of CCD process is to determine the fractional efficiency. Based upon the cutpoint, Lapple then developed an empirical model for the prediction of the collection efficiency for any particle

Table 2. Number of effective turn

Cyclone	Lapple	Observed
1D2D	4	N/A
2D2D	6	6
1D3D	5	6
1D3Dt	2.5	6

size, which is also known as fractional efficiency curve:

$\eta = 1/(1+(d_{pc}/d_{pj})^2)$

d_{pc} = collection efficiency of particles in the jth size range (0<nj<1)

dpj = characteristic diameter of the jth particle size range(in microns).

2.8. Pressure Drop (ΔP)

Cyclone pressure drop is another major parameter to be considered in the process of designing a cyclone system. Two steps are involved in the Lapple approach to estimation of cyclone pressure drop. The first step in this approach is to calculate the pressure drop in the number of inlet velocity heads (Hv) by equation The second step in this approach is to convert the number of inlet velocity heads to a static pressure drop (ΔP) by equation.

There is one problem associated with this approach. "The Lapple pressure drop equation does not consider any vertical dimensions as contributing to pressure drop" (Leith and Mehta, 1973). This is a misleading in that a tall cyclone would have the same pressure drop as a short one as long as cyclone inlets and outlets dimensions and inlet velocities are the same. It has been considered that cyclone efficiency increases with an increase of the vertical dimensions. With the misleading by Lapple pressure drop model.

one could conclude that the cyclone should be as long as possible since it would increase cyclone efficiency at no cost in pressure drop (Leith and Mehta, 1973). A new scientific approach is needed to predict cyclone pressure drop associated with the dimensions of a cyclone.

$Hv = K\ HW/D^2_e$

$\Delta P = ½\ p_g V_i^2 H_v$

Where,

H_v= pressure drop, expressed in number of inlet velocity Heads

K = constant that depends on cyclone configurations and

Operating conditions (K = 12 to 18 for a standard tangential- entry cyclone).

3. CYCLONE EFFICIENCY

3.1. Overall separation efficiency

The overall efficiency is usually the most important consideration in industrial process. Let's us consider the mass balance of solid particle in cyclone. As

explained by Hoffmann and Stein in their book on gas cyclones, Mf, Mc and Me are the mass flow rate of the feed, mass flow rate of particle collected and mass flow rate of escaped particles respectively. Then force balance of solid particle over the cyclone can be denoted by eq. 6

$M_f = M_c + M_e$

The overall separation efficiency can be calculated directly as the mass fraction of feed that is successful.

$\eta = M_c/M_f = 1 - M_e/M_f = M_c/(M_c + M_e)$

3.2. Factors affecting the cyclone collection efficiency

Various factors are observed to affect the cyclone efficiency. An account of some important factors as presented by Schnell and Brown in Air pollution control technology Handbook is presented here.

Inlet velocity is prime factor effecting the pressure drop and hence the cyclone efficiency. Efficiency increases with increase in velocity as centrifugal force increases but this also increases the pressure drop which is not favorable. Also, decreasing the cyclone diameter increases centrifugal force and hence efficiency. Another factor affecting the cyclone efficiency is gas viscosity. With decrease in viscosity, efficiency increases. This is due to reduction in drag force with reduction in viscosity. Decrease in temperature will increase the gas density. One may be tempted to conclude that this will increase efficiency as viscosity decreases. But increase in temperature also decreases the volumetric flow rate and thereby decreasing efficiency. Another

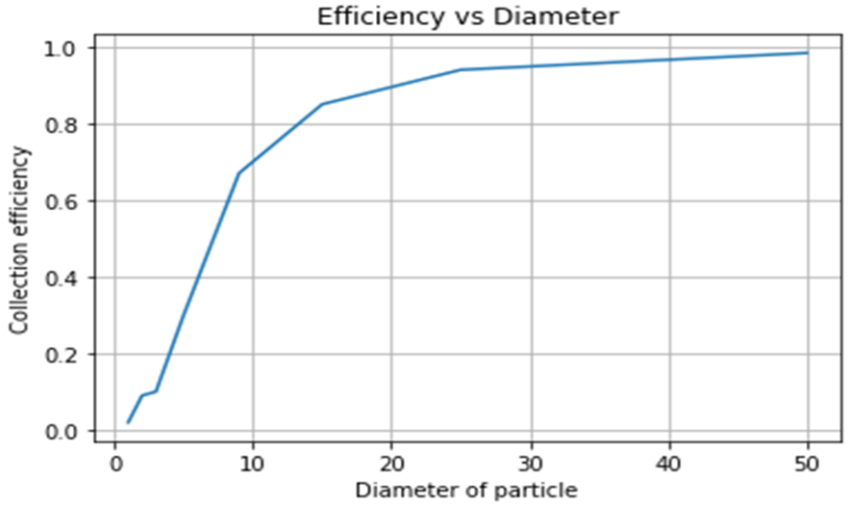

Figure 8. Efficiency vs Diameter

Table 3. Conventional Dimensions

	Dimensions	Ratio	Value(m)
Diameter of cyclone Body (Barrel)	D	D	0.3048
Length of the Body	L_b	2D	0.6090
Length of the Cone	L_c	2D	0.6090
Height of the inlet	H	D/2	0.1524
Width of the inlet	W	D/4	0.0726
Diameter of inlet pipe	d	$A= \pi r^2$	0.1180
Diameter of Gas exit	D_c	D/2	0.1524
Diameter of Dust Outlet	D_d	D/4	0.0726
Length of vortex Finder	S	0.625	0.1905
Length of S_c	S_c	D/8	0.0381
Total length of cyclone	$L_b+ L_c$	4D	1.2192

important factor affecting the efficiency is particle loading. With high loading the particles collide with each other more and results into pushing of particle towards wall. This in turn increases efficiency.

4. EQUIPMENT DESIGN CALCULATIONS

4.1. Standard Cyclone Dimension (Lapple Dimension)

Blower Calculation

Volumetric flow rate of Blower = 0.058 m^3/s

Velocity of Air inlet Duct = Vi= Q/WH

= 0.058/0.0726 * 0.1524

= 5.272 m/s

Dynamic Pressure = ½ pV^2

= ½ *1.22*2.77

P = 16941 pa

Number of Effective Turn

$N_e = 1/H[L_b+ L_c/2]$

$N_e = 1/0.1524[0.609 + 0.609/2]$

$N_e = 6$

Gas Residence time

$\Delta t = \pi DN/V_i$

= 3.14 * 0.3048* 6/5.27

= 1.08 sec

Particle Drift Velocity

$V_t = W/\Delta t$

= 0.0726/1.08

= 0.07055 m/sec

Terminal Drift Transverse Velocity

$V_t = ((p_p - p_a)dp^2V_i^2)/9\mu D$

$= (1602 - 1.22)*(0.0004)^2*(5.27)^2 / 9*0.00183*0.3048$

= 226830.16 m/s

Cut point Diameter

$D_{pc} = [9\mu W/2\pi NVi(p_p - p_a)]^{1/2}$

$= [9*0.0000183*0.0726 / 2*3.14*6*5.27*(1602-1.22)]^{1/2}$

d_{pc} = 6.28 µm

Pressure Drop

$\Delta P = \alpha p V_i^2/2$

$\alpha = 16\ HW/D_e^2$

= 16*0.1524*0.0726/0.0232

= 9.29

ΔP = 9.29 * 1.22*27.772/2

= 157.38 Pa

Power Requirement

$W_f = Q\Delta P$

= 0.058*157.38

W = 9.12 J/sec

Outlet Gas Velocity

$V_o = Q/\pi r_1^2$

= 0.05806/3.14*0.005806

= 3.184 m/sec

Collection Efficiency

$nj = 1/1+(d_{pc}/d_{pj})^2$

Cyclone Efficiency

Overall Collection Efficiency

$M_f = M_c + M_e$

$\eta = M_c/M_f = 1 - M_e/M_f = M_c/(M_c + M_e)$

M_f = 92 +10

η = 92/100 = 1-8/100 = 92/(92 + 80)

= 0.92*100

= 92 %

5. COST ESTIMATION

Cost of cyclone Body = Rs 15000

Cost of Stand = Rs 1000

Cost of labor = Rs 5000

Cost of construction expenses = Rs 5000

Cost of Maintenance = Rs 1000

Testing Cost = Rs 500

Total Cost = Rs 27500

6. CONCLUSION

A prominent problem in calculating the efficiency of cyclone is the effect of flow characters in cyclone. In big cyclones the flow is turbulent and friction factors assumed give good results. This is not true for small cyclones. The flow in small cyclones can be laminar or even transitional. In such case the operational conditions, like velocity, temperature, pressure, viscosity and cyclone diameter, may be of significant importance and their effect changes from cyclone to cyclone. In laminar flow, operating parameters influence cyclone efficiency more than turbulent case. This makes the prediction of efficiency and pressure drop very difficult especially in small cyclone. Most of the models depend on empirical or semi-empirical equations. The models calculate efficiency and predict the cutoff size which corresponds to 50% efficiency. According to Wang et al. cyclone performance is function of geometry and operating parameters of cyclone, as well as particle size distribution of the entrained particulate matter. Several models have been proposed to predict the efficiency of cyclone. It is widely agreed amongst the scientists that cyclone performance is definitely affected by operating parameters and hence they should be included in the modeling. Many theories account for density, gas velocity, viscosity and particle diameter. As far as effect of geometry is considered there is difference in approach for various scientists. Some consider all the geometric parameters where as some consider only few important parameters like inlet and outlet diameter and height in their models. As mentioned, most of the theories consider cut size “d50”, which corresponds to diameter of particle where 50% of particles smaller and 50% of particles greater that that size will be collected. Two most common approaches for calculating efficiency are Force Balance Theory [Lapple] which assumes that terminal velocity is achieved when drag fore and centrifugal force equal each other and the Static Particle Approach [Barth] which considers simple force balance where forces acting on particle are balanced. Various other complicated theories have been proposed but the essentially have their base in one of the two theories.

7. ACKNOWLEDGEMENT

NA.

8. CONFLICT OF INTEREST

The author declares no conflicts of interest.

9. SOURCE(S) OF FUNDING

The author did not require funding.

10. REFERENCES

1. Barth W. 1956. Design and layout of the cyclone separator on the basis of new investigations. Brennstoff-Warme-Kraft 8: 1.
2. Cooper, C.C. and G.C Alley. 1994. Air Pollution Control; A Design Approach. Prospect Heights, Ill.: Waveland Press, Inc.
3. First, M.W., 1950. Fundamental Factors in the Design of Cyclone Dust Collectors. Ph.D. dissertation. Cambridge, Mass.: Harvard University. ¬ Hinds, William C., 1999. Aerosol Technology. New York: John Wiley & Sons.
4. Kaspar, P., K.D. Mihalski and C.B. Parnell, Jr. 1993. Evaluation and development of cyclone design theory. In Proc. 1993 Beltwide Cotton Production Conferences. New Orleans, La. National Cotton Council.
5. Lapple, C. E. 1951. Processes use many collector types. Chemical Engineering 58 (5):144-151 ¬ Leith, D. and W. Licht, 1972. The collection efficiency of cyclone type particle collectors – A new theoretical approach. AIChE Symposium Series 126, 68: 196- 206.
6. A.J. Hoekstra, J.J. Derksen, H.E.A. Van Den Akker An experimental and numerical study of turbulent swirling flow in gas cyclones ¬ L.Y. Hu, L.X. Zhou, J. Zhang, M.X. Shi Studies on strongly swirling flows in the full space of a volute cyclone separator.
7. Shepherd, C.B. and C.E. Lapple. 1940. Flow pattern and pressure drop in cyclone dust collectors.
8. Bayless, G. Kremer and B. Stuart. 2006. CFD simulation of the influence of temperature and pressure on the flow pattern in cyclones. Ind. Eng. Chem. Res. 45:7667–7672.

World Climate Congress 2021
International Journal of Applied Chemical and Biological Sciences
ISSN: 2582-788X

PHARMACOLOGICAL, MOLECULAR, AND ETHNOBOTANICAL APPROACH OF YASUNÍ NATIONAL PARK FOR DEVELOPMENT COMMERCIAL COMMUNITY

Darien Castro *

Laboratorio de Ecosistemas Secos, Facultad de Ciencias Exactas y Naturales. Av. 12 de octubre 1076 y Roca

* For correspondence: dcastro493@puce.edu.ec

Abstract

Given the great debacle caused by the SARS CoV 2 Pandemic, a demand has been seen in the biotechnological field of drug development and the absence of antiviral treatments compounds that put at risk by opening up a possible phenomenon of resistance by mutation in pathogens. For extraction of metabolites of *Piper arboreoum*. Of the 10 diagnosed, 3 had pneumonia and severe respiratory obstruction on day 2 for which they were transferred to El Coca to a center hospital, in the rest due to the lack of access and its remoteness from community centers, had greater reach if not by the community chiefs, unlike the three boarding schools that had access to own river transport and family members in the city. The remaining seven mention an improvement in the evolution of the respiratory symptoms, emphasizing that they were developing dyspnea and respiratory distress said on his own testimony. On the 15th we were notified of a palpable improvement and symptoms gradually disappeared, in our least severe patient after five days. From the 15th to the current date, May 24th, no relapse was pronounced and it has already been examined by brigades of the MSP (Ministry of Public Health) that have taken action in the last week. This was put to test almost spontaneously due to the lack of resources and the benefits of connectivity in line before the national restrictions imposed by the current health emergency of COVID-19.

Keywords: Dyspnea, *Piper arboreoum*, Pneumonia, Respiratory distress, SARS CoV 2

1. INTRODUCTION

1.1. Information about the project and its representative

Given the great debacle caused by the SARS CoV 2 Pandemic, a demand has been seen in the biotechnological field of drug development and the absence of antiviral treatments compounds that put at risk by opening up a possible phenomenon of resistance by mutations in pathogens. The priority during this pandemic is: supply the demand for treatments based on the variety and molecular diversity of compounds, and active ingredients and metabolites found in the flora that inhabit the forests of the Ecuadorian Amazon, take a look in the accessibility and cooperative development of isolated community volunteers for the pharmacological study based on traditional ethnobotany and incidentally give opportunities for training and information dissemination of this organization or civil society in the indigenous communities of the Amazon river.

Analyzing the therapeutic effectiveness of plants through pilot studies and laboratory tests analyzed under optimal conditions and technologies in university facilities. This will serve to a feedback to the ancestral teachings of the communities and link them to development and scientific research for possible future projects and prepare them to demanding system in the academy based on the provision of technical knowledge to indigenous peoples in isolation, giving them the opportunity to apply to higher levels of education through scholarships. Always under the cooperation of Universidad Católica del Ecuador on logistics and equipment issues.

1.2. The international demand of new pharmacological approach

In current alarm of the pandemic, we see a shocking search for innovation in medicine and pharmacology, looking for options without adverse effects and with a low cytotoxic level that guarantees the plenitude and well-being of vulnerable sectors of public health, therefore, the search for sponsorships and business alliances are conspicuous in these times of pandemic and subsequent market rehabilitation to prepare for next major virus outbreaks (Influenza type H, type A) and subsequent public health problems such as neurological disorders and diseases cardiovascular as anxiety patterns,

depression, chronicle stress, myocarditis, rheumatic carditis (Calvo & Cavero 2014).

The regulatory nature of the FDA would be for us a priority entity in the support and cooperation for the development of this project that seeks to promote a population sector rather than a product, to the indigenous and indigenous aboriginal sector, whose knowledge and Ethnobotany millenary knowledge provides us with material to undertake this project (Siren et al. 2020). This market is based on the patent development and scientific analysis, something that is appreciated even more in the university community if it is about social inclusion and scientific and research development in favor of the country and its marginalized areas. In the delimitation of the market we have planned to expose and disseminate this project to level of Iberoamerica, in addition to making it striking in the academic community both for researchers and teachers as well as the youngest and enthusiastic students, who are encouraged to be part of this project and support from their national context these challenges that we carry in our organization. "Innovate without excluding, educate to live".

2. METHODS AND MATERIALS

2.1. Collection and metabolites extraction

About 2.5 kg of plant material was collected. After this, a drying and pressing process was carried out, a taxonomic determination of the specimens was carried out in the QCA Herbarium of the Pontificia Universidad Católica del Ecuador, Quito.

The drying of the leaves would be carried out at about 40 ° C for 3 days in the dryer system of the Botany laboratory at PUCE, reaching a net biomass weight of 0.64kg. After that, the washing was carried out with distilled water and through a screening process to free impurities.

2.2. High efficiency liquid chromatography "HPLC"

The method for the analysis of tl MODEL chemical composition of the sample obtained during the process for obtaining second generation fuel ethanol and calibration were developed by personnel of the company representing Agilent Technologies in Ecuador, Fielquimec, based on applications of Phenomenex brand columns for the analysis of sugars,

fermentation products and fermentation inhibitors.

2.3. Materials Description

2.3.1. High fidelity liquid chromatography equipment

An HPLC will be used as a method for the analysis of the chemical composition of organic extractions by means of equipment calibrated and managed by Agilent Technologies in Ecuador, Fielquimec, based on applications of columns of the Phenomenex brand.

- 1.5 ml capacity vials
- 3 ml syringes
- Filter size 0.22 µm
- Pipettes
- Pipette tips
- Caps with septum for vials
- Rezex Roa Organic Acid column

2.3.2. Reagents

- Sulfuric acid 0.005N
- Type I water
- Certified standard of sugars and fermentation products Supelco brand

2.3.3. Pilot treatment methodology

The 10 residents of the Dicaro community in Orellana diagnosed with COVID19 were called through real time PCR tests and rapid serological tests of Ab / igM, IgG SARS CoV 2 supplied by Amazon Frontlines and COICA as of April 27, with older ages and equal to 60 years, 3 women and 6 men. The treatment was carried out by means of aqueous extract by maceration and infusion of P. arboreum leaves.

Each of the 10 prepared their extract by infusion and maceration in an amount ≥ 2 L of P. arboreum and 2 plants yet to be determined, based on their ancestral and ethnobotanical knowledge, for a week after meals, without additional treatment due the lack of access for public health professionals.

The lack of accessibility in the forest complicates medical follow-up, however, this registration and surveillance has been handled with the pertinent rigor in the face of remoteness by members or community leaders.

2.3.4. Methodology for extraction of metabolites from *Piper arboreoum*

Around 2.5 kg of P. arboreoum was collected, from the vicinity of the Dicaro community in Orellana, Cononaco on the banks of the Yasuní River (-0.9442 S; -

Imagen A. Trabajo de campo y laboratorio de la extracción de Piper arboreum. A1. Recoleccion de material y espécimen. A2. Proceso de secado y tamizaje. A3. Aislamiento de extracto de P. arboreum mediante medio de hexano, diclorometano y acetato de etilo respectivamente.

76.207137 E). After this, a drying and pressing process was carried out, a taxonomic determination of the specimens was carried out in the QCA Herbarium of the Pontificia Universidad Católica del Ecuador, Quito.

The drying of the leaves would be carried out at about 40 ° C for 3 days in the dryer system of the Botany laboratory at PUCE, reaching a net biomass weight of 0.64kg. After that, the washing was carried out with distilled water and through a screening process to free impurities. The maceration process was carried out using a mortar, from there a mixture of 1.7 liters of ethyl alcohol at 70% v / v was made with the plant material and would remain in this way for the next 3 days.

The filtering process was carried out by filter paper and the solid medium or residues and the supernatant or alcoholic medium were obtained. 51.2 g of alcohol extract were obtained which was dissolved in hydrated methanol in a 7: 3 ratios, later the isolation process of active compounds such as Piperidine amide began, liquid / liquid serial solutions were made in 4 l of hexane, 4 l of dichloromethane and 5 l of ethyl acetate (Figueredo et al. 2014).

Thus, 3 media passed through sodium sulfate were obtained for subsequent HPLC analysis.

Piperetine amide

The chemical structure (Figure 1) was determined in comparison with the NMR spectra values in the literature.[18] ^{1}H-NMR ($CDCl_3$, 300 MHz): δ 3.60(4H, m, H-2);1.91 (6H, m, H-3,4,5); 3.58 (4H, m, H-6); 6.20 (1H, d, J = 14.7 Hz, H-8); 7.41 (1H, dd, J = 14.7 and 11.0 Hz, H-9); 6.45 (1H, d, J = 14.7 Hz, H-10); 6.69 (1H, dt, J = 14.7 and 11.0 Hz, H-11); 6.72 (1H, dd, J = 14.7 and 11.0 Hz, H-12); 6.57 (1H, d, J = 14.7 Hz, H-13); 6.98 (1H, d, J = 1.7 Hz, H-2'); 6.78 (1H, d, J = 8.0 Hz, H-5'); 6.88 (1H, dd, J = 8.0 and 1.7 Hz, H-6'); 5.98 (2H, s, OCH_2O). ^{13}C-NMR ($CDCl_3$, 75 MHz): δ 46.74 (C-2); 26.37 (C-3); 24.60 (C-4); 29.94 (C-5); 46.74 (C-6); 165.4 (C-7); 121.59 (C-8); 141.9 (C-9); 130.5 (C-10); 139.86 (C-11); 126.91 (C-12); 135.67 (C-13); 131.6 (C-1'); 105.75 (C-2'); 148.4 (C-3'); 148.4 (C-4'); 108.74 (C-5'); 122.31 (C-6'); 101.46 (OCH_2O).

Table 1. NMR spectrophotometry values based on light diffraction indices in the piperedinamide-forming organic components of Piper arboreum. Diffraction coefficient in MHz and Hz (Comparative results cited by Nacimento et al. 2015)

3. RESULTS AND DISCUSSION

The isolation of compounds such as piperidinamide and possible new compounds will be carried out by HPLC, the results have not yet been obtained due to national quarantine restrictions.

3.1.1. Indigenous pilot treatment

Of the 10 diagnosed, 3 presented pneumonia and severe respiratory obstruction on day 2, so they were transferred to El Coca to a hospital center, in the rest due to lack of access and their distance from community centers, there was no greater reach but by the community chiefs, unlike the three internees who had access to their own river transport and family members in the city. The remaining seven mentioned an improvement in the evolution of the respiratory symptoms, emphasizing that they were developing dyspnea and respiratory distress, according to their own testimony. On day 15, we were notified of a palpable improvement and gradual extinction of symptoms, in our least severe patient at five days. From the 15th to the current date of May 24, 2020, no relapse was pronounced and it has already been examined by brigades of the MSP (Ministry of Public Health) that have taken action in the last week.

In this analysis, we could see some effects in the symptoms and respiratory tract disorders. Neutralization of COVID19 pattern was positive in mild and asymptomatic people, but the severity rate, we could see that the effect is less effective as O_2 saturation rate and pneumonia and inflammatory reactions as COPD symptoms (Gerayeli et al. 2021). We

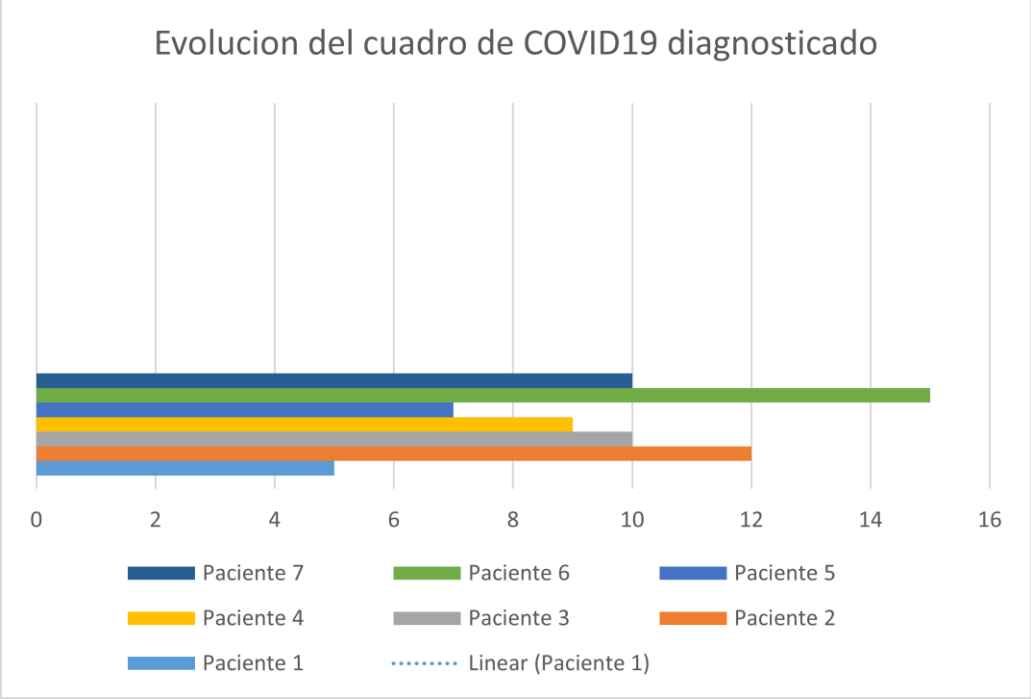

Figure 1. Table of evolution of the picture of COVID19 since the day 27 of April of the taking of real time PCR tests (Time in days).

suggest extensive studies with other plant species in combination due to the traditional extracts that the communities use to infections as viral and bacterial diseases. However, we could see that the combination of some medicine as bronchodilators and compound treatment with corticoids as Dexamethasone and Prednisone. The mix treatment with metabolites from plant extracts and the post therapy in the ICU is the next step to study in future analysis. We couldn't study more variables in the conditions of first emergency alarm in Ecuador in 2020, however we believe that is a great contribution as a review of potential treatments that are unknown in Scientific community. Another species as Uncaria tomentosa (Rubicaceae), Dracontium loretense (Araceae) have analysis in antiviral and immune-stimulator treatments due to compounds and metabolites that promote type 2 immune response and cytotoxic effect in SARS CoV 2 capsule and 3CLpro protease complex proteins and denaturalization (Napolitano et al. 2010; Yepes et al. 2021). Another analysis as HPLC isolation and Agar essays by Antimicrobial susceptibility test (MIC, Mueller-Hinton broth) to proof in isolated samples of lung fluids or blood samples the effect of metabolites (Huang et al.

2014). Many researches in P. arboerum and another Piper species explain a potential as cytotoxic effects and immune-stimulation. As a complement, Piper arboerum extract reduce the detoxication and mortality risk in Bothrops atrox bite (Viperideae) in venom concentration of 50 % v/v (Silva et al. 2017), and the effect as antimicrobial in Streptococcus pyogenes, Staphylococcus aureus and Plasmodium falciparum (Figuerado et al. 2014; Nascimiento et al. 2015; Salehi et al. 2019; Finato et al. 2018). That's the reason because even we can see a potential as inhibitor factor in viral replications and protein synthesis in a variety of virus as Coronaviridae family.

4. ACKNOWLEDGEMENT

NA.

5. CONFLICT OF INTEREST

The author declares no conflicts of interest.

6. SOURCE(S) OF FUNDING

The author did not require funding.

7. REFERENCES

1. Calvo, M. I., & Cavero, R. Y. (2014). Medicinal plants used for cardiovascular diseases in Navarra and their validation from official sources. Journal of ethnopharmacology, 157, 268–273. https://doi.org/10.1016/j.jep.2014.09.047
2. Figuerado et al. 2014, Evaluation of the potential trypanocidal and antileishmanial activities in Piper arboreum (Piperaceae) leaf extract and its fractions, Revista de Ciencias Farmaceuticas Basica e Aplicada 35(1):149-154.
3. Finato, A. C., Fraga-Silva, T. F., Prati, A., de Souza Júnior, A. A., Mazzeu, B. F., Felippe, L. G., Pinto, R. A., Golim, M. A., Arruda, M., Furlan, M., & Venturini, J. (2018). Crude leaf extracts of Piperaceae species downmodulate inflammatory responses by human monocytes. PloS one, 13(6), e0198682. https://doi.org/10.1371/journal.pone.0198682
4. Huang, C. Y., Lai, J. F., Huang, I. W., Chen, P. C., Wang, H. Y., Shiau, Y. R., Cheng, Y. W., Hsieh, L. Y., Chang, S. C., & Lauderdale, T. L. (2014). Epidemiology and molecular characterization of macrolide-resistant Streptococcus pyogenes in Taiwan.

Journal of clinical microbiology, 52(2), 508–516. https://doi.org/10.1128/JCM.02383-13

5. Napolitano, Assunta & Benavides, Angelyne & Pizza, Cosimo & Piacente, Sonia. (2011). Qualitative on-line profiling of ceramides and cerebrosides by high performance liquid chromatography coupled with electrospray ionization ion trap tandem mass spectrometry: The case of Dracontium loretense. Journal of pharmaceutical and biomedical analysis. 55. 23-30. 10.1016/j.jpba.2010.12.035.
6. Gerayeli, Firoozeh V. et al. (2017), COPD and the risk of poor outcomes in COVID-19: A systematic review and meta-analysis, EClinicalMedicine, Volume 33, 10078.
7. Nascimento, Sandra A, Araújo, Emerson A, Da Silva, Janete M, & Ramos, Clécio S. (2015). Chemical Study And Antimicrobial Activities Of Piper arboreum (Piperaceae). Journal of the Chilean Chemical Society, 60(1), 2837-2839. https://dx.doi.org/10.4067/S0717-97072015000100013
8. Salehi, B., Zakaria, Z. A., Gyawali, R., Ibrahim, S. A., Rajkovic, J., Shinwari, Z. K., Khan, T., Sharifi-Rad, J., Ozleyen, A., Turkdonmez, E., Valussi, M., Tumer, T. B., Monzote Fidalgo, L., Martorell, M., & Setzer, W. N. (2019). Piper Species: A Comprehensive Review on Their Phytochemistry, Biological Activities and Applications. Molecules (Basel, Switzerland), 24(7), 1364. https://doi.org/10.3390/molecules24071364
9. Silva, J., Arnóbio Antônio Silva-Junior, Silvana Maria Zucolotto, Matheus de Freitas Fernandes-Pedrosa, (2017), "Medicinal Plants for the Treatment of Local Tissue Damage Induced by Snake Venoms: An Overview from Traditional Use to Pharmacological Evidence", Evidence-Based Complementary and Alternative Medicine, vol. 2017, Article ID 5748256, 52 pages, 2017. https://doi.org/10.1155/2017/5748256.
10. Siren, Anders & Uzendoski, Michael & Swanson, Tod & Negrete, Iván & Gualinga, Emil & Tapia, Andrés & Dahua-Machoa, Alex & Tanguila, Aymé & Santi, Eugenia & Machoa, Dionicio & Andi, Dixon & Santi, Daniel. (2020). Resiliencia contra la pandemia de covid-19 en

comunidades indígenas kichwa en la Amazonía ecuatoriana. Mundos Plurales - Revista Latinoamericana de Políticas y Acción Pública. 7. 101-107. 10.17141/mundosplurales.2.2020.4738.

11. Yepes-Perez, A. F., Herrera-Calderón, O., Oliveros, C. A., Flórez-Álvarez, L., Zapata-Cardona, M. I., Yepes, L., Aguilar-Jimenez, W., Rugeles, M. T., & Zapata, W. (2021). The Hydroalcoholic Extract of Uncaria tomentosa (Cat's Claw) Inhibits the Infection of Severe Acute Respiratory Syndrome Coronavirus 2 (SARS-CoV-2) In Vitro. Evidence-based complementary and alternative medicine: eCAM, 2021, 6679761. https://doi.org/10.1155/2021/6679761

World Climate Congress 2021
International Journal of Applied Chemical and Biological Sciences
ISSN: 2582-788X

Abstracts

World Climate Congress 2021
International Journal of Applied Chemical and Biological Sciences
ISSN: 2582-788X

DIVERSITY PATTERNS OF MONTANE FOREST IN ANDEAN HIGHLANDS AND RECOVERY POTENTIAL IN PATCHES FOREST: A METAPOPULATION APPROACH

Darien Castro [*], Catalina Quintana [#]

Laboratorio de Ecosistemas Secos, Facultad de Ciencias Exactas y Naturales. Av. 12 de octubre 1076 y Roca.

For correspondence: [*] dcastro493@puce.edu.ec, [#] cquintanam@puce.edu.ec

Abstract

The diversity of trees, shrubs and herbs in a remnant of montane forest with an altitude gradient of 2235-3200 m in Imbabura-Ecuador was determined. Species richness was analyzed in six 100 x 5 m transects spread over conserved and disturbed forest areas in order to study the degrees of richness by patch size and its level of connectivity and conservation between patches. In the conserved area, the most dominant and diverse family of trees with the largest basal area was Melastomataceae, while in shrubs, Solanaceae and Piperaceae were the most diverse. In herbaceous, *Trifolium repens* and *Hydrocotile tripartita* were the species with the highest coverage. Subparamo herbaceous species such as *Acaena ovalifolia, Gallium hypocarium* and *Lachemilla orbiculata* were also observed. In the altered zone, the diversity and the basal area in trees is lower compared to the conserved zone. Species like Tibouchina spp. (Melastomataceae) predominate as pioneers. The species *Oreopanax ecuadorensis* (Araliaceae) and Saurauia spp. (Actinidaceae) survive in steep slopes. As for the shrubs, Cestrum spp. and Rubus glaucus were dominant in the transects. In herbaceous, Sporolobus indicus (Poaceae) is the species with the greatest coverage, while *Hydrocotile bondii, Oxalis lotoides* and *Lachemilla orbiculata* are the species with the least coverage. In the future, it is proposed to exercise an agrarian regulation plan to avoid forest degradation by grazing.

Keywords: basal area, connectivity, coverage, Melastomataceae, richness

World Climate Congress 2021
International Journal of Applied Chemical and Biological Sciences
ISSN: 2582-788X

ASSESSING THE POTENTIALS OF DIGITALIZATION AS A TOOL FOR CLIMATE CHANGE ADAPTATION AND SUSTAINABLE DEVELOPMENT IN URBAN CENTRES

Adnan Arshad [1], Muhammad Ashraf [2]

[1] PODA Pakistan & China Agricultural University
[2] University of Baluchistan

For correspondence: adnan.poda@gmail.com

Abstract

Digitalization is a key enabler of sustainable development of cities' socio-economic dynamics with the potential to foster climate-friendly urban environments and societies. High-tech digital devices, platforms and environments are increasingly being deployed to enhance productivity, efficiency and sustainability, and improve overall well-being of urban dwellers. Digitalization is projected to further impact cities in future, transform jobs and trigger life-style changes with far-reaching impacts that will ultimately affect cities' resilience and adaptation capacities. While a growing number of researches have highlighted the significance of digitalization to climate change mitigation such as reducing GHG and CO2 emissions, comprehensive evaluations of the potentials of digitalization as an enabler of climate change adaptation remain scarce. This paper addresses this gap by analysing the current trend in digital revolution in relation to climate change adaptation and examines the likely challenges of digitalization. Our findings reveal the capabilities of digitalization in supporting more effective early warning and emergency response systems, enhancing food and water security, improving power infrastructure performance, enabling citizen engagement and participatory adaptation measures and minimizing the impacts of climatic hazards. Finally, we recommend feasible pathways to overcome present limitations in order to optimize the numerous opportunities offered by digitalization in support of climate change adaptation initiatives.

Keywords: adaptation, climate change, digitalization, sustainable, urban

World Climate Congress 2021
International Journal of Applied Chemical and Biological Sciences
ISSN: 2582-788X

PRODUCTION OF NODULES IN HAIRY ROOT SYMBIOSIS BY ACTINOBACTERIEAE COLONY AS IMMUNE AND NITRIFICATION ENHANCER

Darien Castro *

Laboratorio de Ecosistemas Secos, Facultad de Ciencias Exactas y Naturales. Av. 12 de octubre 1076 y Roca.

* For correspondence: dcastro493@puce.edu.ec

Abstract

Nitrogen-fixing organisms are usually associated with bacteria and fungi colonies, which are generally located in nodules of Fabales roots. Frankia spp. allows soil degradation and in turn develops a plant-microorganism association. This mutualism development has a great capacity as a biological control agent, since it can regulate and prevent pathogens. Actinomycetes can contribute greatly to supplant fungicides and can improve crop yield. For the field phase, roots of Coriaria microphylla were collected by scraping nodules on the roots. This medium was heated for 1 minute and Murashige and Skoog medium (MS) 1% was dissolved in this medium; this result was placed in previously sanitized Petri dishes. The plants were placed in cotton and water with diluted MS medium was placed after 4 days. As results, in the first control phase: from week 1 to week 5 of registration, there was a stagnation in the development of the outbreak. However, increased leaf size and phototropism was noted in plants inoculated with Frankia spp., this is due to a possible immune response from phytocytokines. In the generation of nodular primordium, it was observed that the development of hairy roots from the inoculated area has the same response than specialized agar cultures such as Hoagland medium, that's a signal of plasticity. In plants without actinomycetes, galls were presented, this is due to the following factors: Immunological deficiency and pattern of susceptibility to parasitic infections, and stimulation of cytokines, and resistance to biotic or abiotic stress are seen in arbuscular mycorrhizae.

Keywords: Actinobacterieae, nodules roots, phytocytokine

World Climate Congress 2021
International Journal of Applied Chemical and Biological Sciences
ISSN: 2582-788X

DEVELOPMENT OF CYTOGENETIC MARKERS FOR IDENTIFICATION OF POLYMORPHIC INVERSION KARYOTYPE IN DIPLOID CELLS OF *ANOPHELES MESSEAE* (CULICIDAE) MALARIA MOSQUITO

Calderon R. Ximena *, Artemov Gleb

Department of Cytology and Genetics, Biological Institute, National Research Tomsk State University (NS TSU), Lenin Ave, 36, Tomsk, Tomsk Oblast, 634050.

* For correspondence: ximena.calderon0227@gmail.com

Abstract

Anopheles messeae is a member of the Maculipennis group of malaria mosquitoes that has the most northern distribution among other members of the group. It shows a high genetic diversity, which is based on the high polymorphism that this species has, allowing a high plasticity of adaptation. In this study, PCR-amplified DNA probes for fluorescence in situ hybridization (FISH) were designed based on An. messeae genome. The DNA probe obtained by microdissection procedures from the breakpoint region was labelled in a DOP-PCR reaction. to verify our probe, we also identify inversions in polythene chromosomes. Population analysis was performed from specimens collected in Kolarovo (Tomsk-Russia) from imaginal disks of 4th stage larvaes for mitotic chromosomes and salivary glands for polythene chromosomes. As result we confirm the suitability of several PCR amplified probes that were detected in the chromosomes of An. messeae using FISH, (Fig 1, and Fig 2) The breakage and transposition of the labelled region in :2R00, 2R11, XL11, 3R00, 3R11, 3L00, 3L11 chromosomes demonstrating the utility of DNA- probe method for detection of inversions in mitotic chromosomes, being useful for identification inversion variants in non-polytene cells, also cytogenetic analysis determined inversion polymorphism in natural populations of An. messeae related to the adaptation of this species.

Keywords: anopheles, mosquito, cytogenetic map, inversion polymorphism, physical mapping